HHS Public Access

Author manuscript

Clin Cancer Res. Author manuscript; available in PMC 2021 September 15.

Published in final edited form as:

Clin Cancer Res. 2021 March 15; 27(6): 1792–1806. doi:10.1158/1078-0432.CCR-20-2483.

Attenuation of SRC kinase activity augments PARP inhibitor–mediated synthetic lethality in *BRCA2*-altered prostate tumors

Goutam Chakraborty[1,*,#], **Nabeela Khan Patail**[1,5,*], **Rahim Hirani**[1], **Subhiksha Nandakumar**[2], **Ying Z. Mazzu**[1], **Yuki Yoshikawa**[1], **Mohammad Atiq**[1,6], **Lina E. Jehane**[1], **Konrad H. Stopsack**[1], **Gwo-Shu Mary Lee**[3], **Wassim Abida**[1], **Michael J. Morris**[1], **Lorelei A. Mucci**[4], **Daniel Danila**[1], **Philip W. Kantoff**[1,#]

[1]Department of Medicine, Memorial Sloan Kettering Cancer Center, New York, NY

[2]Center for Molecular Oncology, Memorial Sloan Kettering Cancer Center, New York, NY

[3]Dana-Farber Cancer Institute, Boston, MA

[4]Department of Epidemiology, Harvard T.H. Chan School of Public Health, Boston, MA

Abstract

Purpose: Alterations in DNA damage repair (DDR) pathway genes occur in 20–25% of men with metastatic castration-resistant prostate cancer (mCRPC). Although poly (adenosine diphosphate [ADP]-ribose) polymerase inhibitors (PARPi) have been shown to benefit men with mCRPC harboring DDR defects due to mutations in *BRCA1/2* and *ATM,* additional treatments are necessary because the effects are not durable.

Experimental Design: We performed transcriptomic analysis of publicly available mCRPC cases, comparing *BRCA2*-null to *BRCA2* wild type. We generated *BRCA2*-null prostate cancer cells using CRISPR/Cas9 and treated these cells with PARPi and SRC inhibitors. We also assessed the antiproliferative effects of combination treatment in 3D prostate cancer organoids.

Results: We observed significant enrichment of the SRC signaling pathway in *BRCA2*-altered mCRPC. *BRCA2*-null prostate cancer cell lines had increased SRC phosphorylation and higher

Corresponding authors: Philip W. Kantoff or Goutam Chakraborty, Memorial Sloan Kettering Cancer Center, 1275 York Avenue, New York, NY 10065, USA, Tel: 212-639-5851, Fax: 929-321-5023, kantoff@mskcc.org, chakrabg@mskcc.org.

[5]Current address: Department of Medicine, Stony Brook University Hospital, Stony Brook, NY

[6]Current address: Division of Hematology-Oncology, Baylor College of Medicine, Houston, TX

[#]co-corresponding authors

[*]co-first authors of this article

Author contributions:

Conception and design: G Chakraborty, N Khan Patail, PW Kantoff

Development of methodology: G Chakraborty, N Khan Patail, R Hirani, GM Lee, W Abida

Acquisition of data (provided animals, acquired and managed patients, provided facilities, etc.): G Chakraborty, N Khan Patail, R Hirani, YZ Mazzu, Y Yoshikawa, M Atiq, LE Jehane

Analysis and interpretation of data (eg, statistical analysis, biostatistics, computational analysis): S Nandakumar, KH Stopsack, M Morris, LA Mucci, D Danila

Writing—original draft: G Chakraborty, N Khan Patail, R Hirani, S Nandakumar, YZ Mazzu, PW Kantoff

Writing—review and editing: G Chakraborty, Y Yoshikawa, M Atiq, LE Jehane, KH Stopsack, GM Lee, W Abida, MJ Morris, LA Mucci, D Danila, PW Kantoff

Administrative, technical, or material support (ie, reporting or organizing data, constructing databases): G Chakraborty, S Nandakumar

Study supervision: G Chakraborty, PW Kantoff

Final approval of the manuscript version submitted for publication: all authors.

The other authors have no potential conflicts of interest to disclose.

sensitivity to SRC inhibitors (eg, dasatinib, bosutinib, and saracatinib) relative to wild-type cells. Combination treatment with PARPi and SRC inhibitors was antiproliferative and had a synergistic effect in *BRCA2*-null prostate cancer cells, mCRPC organoids, and Trp53/Rb1-null prostate cancer cells. Inhibition of SRC signaling by dasatinib augmented DNA damage in *BRCA2*-null prostate cancer cells. Moreover, *SRC* knockdown increased PARPi sensitivity in *BRCA2*-null prostate cancer cells.

Conclusions: This work suggests that SRC activation may be a potential mechanism of PARPi resistance and that treatment with SRC inhibitors may overcome this resistance. Our preclinical study demonstrates that combining PARPi and SRC inhibitors may be a promising therapeutic strategy for patients with *BRCA2*-null mCRPC.

Keywords

PARP inhibitor; SRC inhibitor; *BRCA2* deletion; castration-resistant prostate cancer; combination treatment

INTRODUCTION

Metastatic castration-resistant prostate cancer (mCRPC) is lethal and incurable (1). Treatment options for patients with mCRPC have expanded significantly, but de novo and acquired resistance occurs frequently. Large-scale genomic studies (2,3) have revealed a high degree of genomic instability (4) and frequent alterations in DNA damage repair (DDR) genes (2,5) in patients with mCRPC. Alterations in *BRCA2,* a hallmark DDR and cancer susceptibility gene, are also prevalent in men with advanced prostate cancer (PC) (6,7), including homozygous and heterozygous *BRCA2* deletions (8). *BRCA2* alterations, especially loss-of-function mutations, have been observed in a higher proportion of men with mCRPC and are associated with a worse prognosis (5,6). In the PROREPAIR-B mCRPC cohort, *BRCA2* germline mutations were reported to negatively affect outcome (9). However, the molecular mechanisms through which *BRCA2* loss accelerates PC progression are poorly understood.

A significant fraction of localized PC and mCRPC harbor *BRCA2* deletions (10). *BRCA2* is frequently co-deleted with *RB1,* and co-deletion was significantly enriched in mCRPC and was associated with higher genomic instability. *BRCA2/RB1* co-deletion impaired DNA repair, induced castration resistance, and augmented an epithelial-mesenchymal transition–like aggressive phenotype (10). Beltran et al. reported *BRCA2* deletions in 30–50% of mCRPC and in *TP53*/*RB1*-deficient neuroendocrine PC (8). They also showed that alterations in DDR genes (primarily *BRCA2*) were significantly associated with poor overall survival ($P = 0.001$) (8). These data suggest that *BRCA2* deletion leads to aggressive PC and indicate that the underlying signaling pathways need to be investigated.

Poly (ADP-ribose) polymerase (PARP) inhibitors (PARPi) cause single-strand break accumulation (11) and synthetic lethality in DDR-impaired tumors due to mutated or deleted *BRCA1/2* (12). PARPi are approved for the treatment of ovarian cancer, breast cancer, and PC (13). In a phase II trial in 49 patients with mCRPC, 16 (33%) showed a significant response to olaparib. Importantly, 88% of those who responded to olaparib harbored

homologous recombination repair defects due in large part to *BRCA2* and *ATM* alterations (14). The landmark TRITON2, TOPARP-B, and PROfound 3 trials showed that germline and somatic *BRCA2* alterations were associated with increased response to olaparib and rucaparib (15–18). Recent data have also shown that patients with loss of *BRCA1/2* in multiple cancers, including PC, experienced clinical benefit with PARPi (19). In TRITON2, patients with *BRCA1/2* alterations treated with rucaparib had a 52% prostate-specific antigen response rate and a 43.9% response rate in patients with measurable disease. The duration of response was ≥ 6 months in 15 (56%) of the 27 patients with confirmed objective responses (20). However, resistance is common, resistance mechanisms are poorly understood (21), and treatment modalities for patients resistant to PARPi are limited. Combination strategies that are well tolerated and have a synergistic effect are needed.

Increasing evidence has connected oncogenic nonreceptor tyrosine kinase SRC activity with aggressive PC (22). Phosphoproteomic analysis of mCRPC showed that SRC is one of the most activated kinases (23). *Src* knockout reduced primary tumor growth and metastasis (24). Although SRC activation is known to be required for checkpoint recovery termination and SRC inhibition delays G2 DNA damage checkpoint recovery following DNA double-strand break (DSB) repair (25,26), the role of SRC in DDR is incompletely understood.

We analyzed the transcriptomic profile of *BRCA2*-deleted mCRPC, and, for the first time, demonstrated that SRC pathway activation is directly associated with *BRCA2* loss. We observed strong SRC activation and increased dasatinib sensitivity in *BRCA2*-knockout PC cells. We demonstrated that the combined use of PARPi and SRC inhibitors in *BRCA2*-deleted PC cell lines has a synergistic effect on cell viability. We found that *SRC* knockdown increases PARPi sensitivity, indicating that SRC activation may be important in PARPi resistance. Our study suggests that there may be significant promise in exploring combined inhibition of PARP and SRC in *BRCA2*-altered mCRPC as well as in *TP53*/*RB1*-altered neuroendocrine PC.

METHODS

Bioinformatic analysis of clinical cohorts

The association between *BRCA2* genomic deletion (heterozygous and homozygous) and disease progression in various PC clinical cohorts was analyzed in cBioPortal (27,28). The transcriptomic profile of tumors with *BRCA2* alteration was generated in cBioPortal and pathway analysis for oncogenic and hallmark signature performed using gene set enrichment analysis (GSEA). Ten PC cohorts were used in this study (Supplementary Table S1). Graphs and Kaplan-Meier survival curves were plotted using GraphPad Prism (version 7, La Jolla, CA).

Cell culture

Cells were purchased from ATCC (Manassas, Virginia) unless otherwise specified in Supplementary Table S2. LNCaP, DU145, 22RV1, and TRAMP-C2 were purchased from ATCC (Manassas, Virginia). PC3M cells were provided by Raymond C. Bergan (Knight Cancer Institute, Oregon Health & Science University, Portland, OR). Cells were cultured in

RPMI1640 (LNCaP, 22RV1 and PC3M) or DMEM (DU145, TRAMP-C2) media supplemented with 10% FBS, 2 mM L-glutamine, and 1X antibiotic/antimycotic (Gemini Bio-Products, Sacramento, CA) at 37°C in 5% CO_2. The LNCaP-abl cell line was provided by Zoran Culig (Innsbruck Medical University, Innsbruck, Austria) and was maintained in phenol red–free RPMI1640 media supplemented with 10% charcoal-stripped serum, 2 mM L-glutamine, and 1X antibiotic/antimycotic. RWPE1 cells were obtained from ATCC and cultured in keratinocyte serum-free medium (Thermo Fisher Scientific, Waltham, MA) at 37°C in 5% CO_2. Prostate organoids derived from patients with mCRPC were provided by Dr. Yu Chen (Memorial Sloan Kettering Cancer Center [MSK], New York, NY) and cultured as described previously (29). Cells were acquired between 2017 and 2019; in general, there were between two and six passages between collection and thawing. Cells were authenticated by human short tandem repeat profiling at the MSK Integrated Genomics Operation Core Facility in December 2017 and June 2019. Mycoplasma testing was performed at the MSK Antibody & Bioresource Core Facility using the MycoAlert™ PLUS Assay in January 2019. CRISPR/Cas9-mediated *BRCA2* knockout was performed in LNCaP as described earlier (10). gRNA sequences are shown in Supplementary Table S2. Single cell–derived *BRCA2* knockout LNCaP clones were analyzed by Sanger sequencing at the MSK Gene Editing & Screening Core Facility.

Western blot

Cells were washed with Hank's Balanced Salt Solution (HBSS) and lysed in RIPA (50 mM TRiS-HCl pH 7.4, 150 mM NaCl, 1 mM EDTA, 1% Triton X-100, 1% sodium deoxycholate, and 0.1% SDS) supplemented with protease and phosphatase inhibitors (Thermo Scientific). Protein concentrations were measured using the Bradford protein assay. Western blot was performed using specific antibodies (Supplementary Table S2). Freshly prepared cell lysates were used for BRCA2 western blot as described earlier (10).

RNA extraction and qPCR

RNA isolation was performed using the Direct-zol RNA Kit (Zymo Research, Irvine, CA) and reverse transcribed with qScript cDNA SuperMix (Quantabio, Beverly, MA). cDNA corresponding to approximately 10 ng of starting RNA was used for one reaction. qPCR was performed with Taqman Gene Expression Assay (Applied Biosystems, Waltham, MA). GAPDH was used as an internal control. Taqman probe sequences are shown in Supplementary Table S2.

Cell viability assay

Cell viability was measured by MTT (3-[4,5-dimethylthiazol-2-yl]-2,5-diphenyl tetrazolium bromide; Invitrogen) assay. Cells were plated in 96-well plates in complete media (2.5×10^3 for LNCaP, 22RV1, LNCaP-abl, and RWPE1, 1×10^3 cells for PC3M, and 5×10^3 for MSKPCa1 and MSKPCa3). 96-well plates were precoated with 50 μg/mL collagen I (rat tail; Thermo Scientific) for MSKPCa1 and MSKPCa3 cells. Cells were treated with DMSO or indicated inhibitors at day 0 and at day 3 unless otherwise mentioned. After indicated times, cells were incubated in 0.5 mg/mL MTT for 2 hours at 37°C. MTT crystals were dissolved in isopropanol and absorbance was measured in a plate reader at 570 nM.

Drug synergy analysis

PC3M and LNCaP-abl cells were treated with PARPi (olaparib and talazoparib) and dasatinib alone or in combination for 5 days. Drugs were added to the cells at day 0 and at day 3. The combination index–isobologram equation was used to quantitatively calculate the drug interaction. The Chou-Talalay method (Compusyn) is a standardized definition for synergy in drug combinations and is based on the median-effect equation. The different identifications are based on the combination index. The dose response and combination index–effect plots show the combinational effect of indicated drugs on cell proliferation, where combination index < 1 indicates synergism, combination index = 1 is additive, and combination index > 1 indicates antagonism (30).

DNA damage assay

Cells were treated with dasatinib (0.3 μM) for 24 hours. DNA damage was quantified using MUSE multi-color DNA damage kit (Luminex; **MCH200107**) in Guava MUSE cell analyzer system according to the manufacturer's instructions. Experiments were performed in triplicate.

Comet assay

1×10^5 LNCaP scrambled and *BRCA2* knockout (pooled population and single cell–derived clones) cells were incubated in media supplemented with dasatinib (0.3 μM) for 24 hours. Comet assay was performed using the Comet assay kit (Abcam; ab238544) according to the manufacturer's instructions. Photographs were captured under fluorescence microscopy.

Mouse strains

Male wild-type C57BL/6J mice and C57BL/6-Tg(TRAMP) mice were purchased from The Jackson Laboratory. Normal prostates (from wild-type C57BL/6J mice) and localized prostate tumors (from C57BL/6-Tg(TRAMP) mice) were isolated from 30-week old mice and fixed in 4% paraformaldehyde followed by paraffin embedding, sectioning, and staining using indicated antibodies. All animal experiments were performed in the MSK Research Animal Resource Center Core Facility according to the Institutional Animal Care and Use Committee protocol.

3D Matrigel organoid assays

Organoid assays were performed as described earlier (31). Briefly, PC3M, LNCaP-abl, MSKPCa1, and MSKPCa3 cells were detached using Accutase (Innovative Cell Technologies, San Diego, CA), collected using 70-μm cell strainers, counted (1×10^3 cell/well for PC3M cells and 5×10^3 cell/well for LNCaP-abl, MSKPCa1, and MSKPCa3 cells), and resuspended in prostate organoid media (29) and mixed with Matrigel Membrane Matrix (Fisher Scientific CB-40234C) in a 1:1 ratio. The cell and Matrigel mixtures were plated on ultra-low attachment plates and allowed to grow for the indicated times. Detailed schematic representations of the organoid experiments are shown in Supplementary Figure S6A. Organoids were counted and photographed using GelCount colony counter (Oxford Optronix, Abingdon, England).

Statistical analysis

Results are reported as mean ± standard deviation, unless otherwise noted. Comparisons between groups were performed using an unpaired two-sided Student's *t* test, unless noted. Graphs were generated with GraphPad Prism (version 7.0 GraphPad Software, Inc, La Jolla, CA).

RESULTS

BRCA2 deletion in mCRPC is associated with enhanced SRC activation

To identify the frequency of *BRCA2* alterations in PC, we analyzed data from cBioPortal for Cancer Genomics (27,28). We observed that *BRCA2* is frequently deleted in localized PC, mCRPC, and neuroendocrine PC, with heterozygous/shallow deletions more frequent than homozygous/deep deletions (Supplementary Fig. S1A). Biochemical recurrence was more common in patients with *BRCA2* deletions than in patients with wild-type *BRCA2* (Supplementary Fig. S1B; P=9.35e-7; Q=1.964e-5). The Gleason scores of patients with *BRCA2* deletions were significantly higher than the Gleason scores of patients with wild-type *BRCA2* (Supplementary Fig. S1C; P=1.902e-5, Q=3.551e-4). The proportion of metastatic cases was significantly higher in patients with homozygous or heterozygous *BRCA2* deletions than in patients with wild-type *BRCA2* (Supplementary Fig. S1D; $P <$ 10e-10, $Q <$ 10e-10). These data suggest that *BRCA2* deletion may be associated with aggressive PC.

To investigate the signaling pathways associated with *BRCA2-deleted* mCRPC, we used publicly available data from the Kumar cohort (32). *BRCA2* deletions were found in 56% of mCRPC cases (Fig. 1A). We compared gene expression between patients with homozygous and heterozygous deletions of *BRCA2* and patients with wild-type *BRCA2* (Fig. 1B, Supplementary Table S3). We performed GSEA and found increased expression of several important oncogenic signaling pathways (eg, E2F3, KRAS, and EZH2) and significant enrichment of the oncogenic tyrosine kinase SRC signaling pathway (normalized enrichment score [NES] = 1.8; P = 0.003, false discovery rate [FDR] = −0.05; Fig. 1C,D; Supplementary Table S3). We also performed GSEA comparing cases with *BRCA2* homozygous deletion to cases with wild-type *BRCA2,* cases with *BRCA2* heterozygous deletion to cases with wild-type *BRCA2*, and cases with *BRCA2* homozygous deletion to cases with *BRCA2* heterozygous deletion (Supplementary Fig. S1E–G). We observed SRC signaling pathway enrichment in cases with homozygous *BRCA2* deletion compared to cases with wild-type *BRCA2* (NES = 1.3; P = 0.046, FDR = 0.073; Supplementary Table S3) and in cases with heterozygous *BRCA2* deletion compared to cases with wild-type *BRCA2* (NES= 1.55; P = 0.003, FDR = 0.02; Supplementary Table S3). The SRC pathway was not enriched when cases with homozygous and heterozygous *BRCA2* deletions were compared (Supplementary Table S3).

We also performed the hallmark pathway analysis using GSEA and found that attenuation of androgen signaling was associated with *BRCA2*-deleted mCRPC (Fig. 1E,F; Supplementary Table S3). To identify drug targets associated with *BRCA2*-deleted mCRPC, we performed ToppGene suite analysis (33) of the upregulated transcriptome. The potent SRC inhibitor

dasatinib was one of the top drug targets associated with the *BRCA2-deleted mCRPC* transcriptome (Fig. 1G). Our data suggest that SRC pathway activation may be associated with *BRCA2*-deleted mCRPC.

Increased *SRC* phosphorylation in BRCA2-null PC cells

To investigate the direct effect of *BRCA2* loss on SRC pathway activation, we used CRISPR/Cas9 to generate *BRCA2*-knockout LNCaP cells, a hormone-dependent human PC cell line with wild-type *BRCA2* (10). LNCaP cells transfected with nontargeting/scrambled gRNA served as a control as described previously (10). We confirmed *BRCA2* loss in *BRCA2* gRNA–transduced cells and observed increased SRC phosphorylation at tyrosine-416 (Y416) in cells transduced with all gRNAs targeting *BRCA2* compared to cells transduced with the control (scrambled) gRNA (Fig. 2A, Supplementary Fig. S2A). SRC phosphorylation at Y416, which is in the activation loop of the kinase domain, is a key step leading to high SRC activity (34). We also assessed whether *BRCA2* loss induced activation of other signaling pathways by western blot, particularly those pathways that we found to be enriched in *BRCA2*-null mCRPC (Fig. 1C,D). We did not observe increased phosphorylation of ERK (KRAS pathway) and JNK or induction of EZH2 in *BRCA2*-knockout cells compared to control cells (Fig. 2B). We did observe activation of the ATR-ATF2 pathway, indicating the induction of DNA damage in *BRCA2*-null LNCaP cells. Our data also showed increased phosphorylation of FAK, a downstream target of SRC (35), in *BRCA2*-knockout cells compared to control cells, further indicating that the SRC signaling pathway is activated in *BRCA2*-null PC cells (Fig. 2B). We also observed induction of AKT phosphorylation (PTEN pathway) in *BRCA2*-knockout cells relative to control cells.

To demonstrate that *BRCA2* loss induces SRC phosphorylation in the absence of any exogenous factors, we assessed SRC phosphorylation in cells grown in serum-free media and then treated with epidermal growth factor (EGF). Levels of SRC phosphorylation were higher in the serum-starved *BRCA2*-knockout cells than in the control cells, even without EGF treatment (Supplementary Fig. S2B). Increased SRC phosphorylation was observed in *BRCA2*-null LNCaP-abl, DU145, and PC3M cells, which harbor *BRCA2* heterozygous deletions (10) and low *BRCA2* mRNA levels (Supplementary Fig. S2C), compared to LNCaP cells (Fig. 2C). RNAi-mediated knockdown of *SRC* inhibited FAK phosphorylation in *BRCA2*-null LNCaP-abl cells, indicative of SRC-mediated FAK activation in these cells (Supplementary Fig. S2D). Our data indicate that loss of *BRCA2* is sufficient to induce SRC activation in PC cells.

We next examined the effects of SRC inhibitor treatment on *BRCA2*-null PC cells. As expected, SRC-Y416 phosphorylation was reduced in *BRCA2*-null PC3M and LNCaP-abl cells treated with dasatinib (Supplementary Fig. S2E,F). However, treatment with dasatinib did not inhibit AKT phosphorylation in LNCaP-abl cells (Supplementary Fig. S2F). We observed that a pooled population of *BRCA2*-null LNCaP cells (LNCaP *BRCA2*-gRNA 2) exhibited enhanced sensitivity to dasatinib compared to cells transduced with a scrambled/nontargeting gRNA (Fig. 2D, top). We also generated single cell–derived clones from *BRCA2*-knockout cells (LNCaP *BRCA2*-gRNA-cl7) and confirmed *BRCA2* loss by CRISPR sequencing (wild-type *BRCA2* elimination > 99%; Supplementary Table S4).

Dasatinib reduced the viability of LNCaP *BRCA2*-gRNA2-cl7 cells (Fig. 2D, top). There was no significant difference in cell viability with dasatinib treatment between the pooled cells and the single cell–derived clones. Importantly, we observed that dasatinib also suppressed the elongated morphology of control cells, LNCaP *BRCA2*-gRNA 2 cells, and LNCaP *BRCA2*-gRNA-cl7 cells (Fig. 2D, bottom). Similarly, other SRC-specific inhibitors bosutinib (SKI606) and saracatinib (AZD-0530) strongly reduced the viability of *BRCA2*-null LNCaP cells (LNCaP *BRCA2*-gRNA 2) cells compared to control cells (Fig. 2E). However, inhibition of AKT by ipatasertib did not have a significant inhibitory effect on cell viability in *BRCA2*-null LNCaP cells compared to scrambled LNCaP cells (Fig. 2F). These data indicate that inhibition of the SRC pathway reduces the viability and invasiveness of these PC cell lines.

We assessed whether increased levels of SRC phosphorylation were associated with poor outcomes in patients with localized PC. Increased SRC-Y416 phosphorylation was modestly but not statistically significantly associated with decreased disease-free survival in The Cancer Genome Atlas (TCGA) cohort of primary PC (P_{trend} = 0.0546; 95% confidence interval [CI], 0.9319 to 3.619; Fig. 2G). We were unable to detect an association between levels of SRC-Y527 phosphorylation or levels of SRC and disease-free survival in the same cohort (Supplementary Fig. S2G,H). We did not detect a significant association between SRC-Y416 phosphorylation and Gleason grade (Supplementary Fig. S2I, top) or between *BRCA2* deletion and SRC-Y416 phosphorylation levels (Supplementary Fig. S2I, bottom). To further understand the role of SRC activation in localized PC, we compared gene expression between patients with high SRC activation (top quartile; Fig. 2G) and those with low SRC activation (bottom quartile; Fig. 2G) and performed GSEA. We found enrichment of several oncogenic signaling pathways, including induction of the PIGF pathway (Fig. 2H). Previous studies have shown that placental growth factor/PIGF, a secreted stromal factor that can induce SRC activation (36), plays an important role in cancer progression (37). Taken together, these data suggest that SRC Y416 phosphorylation may be associated with primary PC progression; however, additional oncogenic alterations may lead to SRC activation in primary PC.

Synergistic effect of PARPi and dasatinib in *BRCA2*-null PC cells

Recently, PARPi have shown promise in patients with mCRPC harboring DDR pathway defects—in particular, but not exclusively, *BRCA2*-altered tumors—leading to FDA approval (14–18). Despite responses, resistance is common, and treatment modalities for patients resistant to PARPi are limited. Given these data, we hypothesized that combined inhibition of SRC and PARP could be a therapeutic option for patients with *BRCA2* alterations.

To study the effects of dasatinib in combination with PARPi, we used CompuSyn synergism/antagonism analysis (30). Briefly, cells were treated with increasing concentrations of dasatinib and either olaparib or a PARPi that exhibits higher PARP1 trapping, talazoparib. We observed that dasatinib acted synergistically (combination index < 1) with both talazoparib and olaparib in *BRCA2*-null LNCaP-abl and PC3M cells (Fig. 3A,B; Supplementary Fig. S3A,B). Although the dasatinib-talazoparib combination was strongly

synergistic in both LNCaP-abl and PC3M cells, the synergistic effect of the dasatinib-olaparib combination was stronger in PC3M cells than in LNCaP-abl cells (Fig. 3A,B, Supplementary Fig. S3A,B).

We also examined the effect of combination treatment on the viability of LNCaP-abl (0.3 μM dasatinib and 0.03 μM talazoparib alone or in combination) and PC3M cells (0.3 μM dasatinib and 3.0 μM olaparib alone or in combination). The combination of dasatinib with PARPi significantly reduced cell viability over treatment with either drug alone (Supplementary Fig. S3C,E). In particular, treatment of LNCaP-abl cells with dasatinib alone had no effect on cell viability, but the combination of talazoparib and dasatinib significantly reduced cell viability (Supplementary Fig. S3C).

We next assessed the effect of combination treatment on the viability of LNCaP *BRCA2*-gRNA 2 cells over time. We treated cells with 0.3 μM dasatinib and 3.0 μM olaparib, the concentrations that produced a synergistic effect on cell viability. Combination treatment of control/scrambled LNCaP cells reduced cell viability, but the effect was modest compared to olaparib treatment alone (Fig. 3C). We observed a significant reduction in the viability of LNCaP *BRCA2*-gRNA 2 cells treated with the combination of dasatinib and olaparib. Treatment with either drug alone only partially inhibited viability (Fig. 3C,D). Olaparib alone did not alter the invasive elongated morphology of LNCaP *BRCA2-gRNA* 2 cells (Fig. 3E). These data demonstrate that combination treatment inhibits cell viability and suppresses the invasive elongated morphology of *BRCA2*-knockout PC cells.

To further confirm the effect of dual inhibition of SRC and PARP on the viability of *BRCA2*-null PC cells, we treated LNCaP-abl cells with bosutinib (0.3 μM) and saracatinib (0.3 μM) alone and in combination with talazoparib (0.03 μM) for 7 days (Fig. 3F, Supplementary Fig. S3D). We found that the combined inhibition of SRC and PARP strongly reduced the viability of LNCaP-abl cells over the inhibition of SRC or PARP alone (Fig. 3F, Supplementary Fig. S3D).

Recent clinical data have shown that patients with mCRPC with DDR mutations (particularly *BRCA2*) respond to platinum-based chemotherapy (38). To investigate whether inhibition of SRC increases the efficacy of platinum-based therapy, we treated cells (LNCaP-scrambled and LNCaP *BRCA2*-gRNA 2) with 0.3 μM dasatinib and 0.1 μM cisplatin for 5 days (Fig. 3G,H). We observed a strong reduction in the viability of LNCaP *BRCA2*-gRNA 2 cells treated with the combination of dasatinib and cisplatin, while treatment with either drug alone only partially inhibited viability (Fig. 3G,H). Taken together, our data suggest that SRC inhibitors can increase the growth inhibitory effect of both PARP and platinum-based therapy in *BRCA2*-null PC cells.

Dasatinib induces DNA damage in BRCA2-null PC cells

To test our hypothesis that dasatinib induces DNA damage, we treated PC3M cells with dasatinib for 24 hours and assessed DNA damage by phospho-γH2Ax and phospho-ATM as measured by flow cytometry. Dasatinib-treated PC3M cells had increased γH2AX phosphorylation relative to DMSO-treated cells, indicative of defective DSB repair (Fig.

4A). There was a modest increase in ATM phosphorylation in dasatinib-treated cells, indicating that SRC phosphorylation inhibition induces DNA damage (Fig. 4A).

To determine whether *BRCA2* loss affected dasatinib-induced DNA damage, we treated LNCaP *BRCA2*-gRNA2-cl7 and control cells with dasatinib (0.3 μM) for 24 hours. Dasatinib induced DNA damage in *BRCA2*-knockout cells but not control cells (Fig. 4B,C). We also examined DNA damage in dasatinib-treated cells using the comet assay, which directly measures DNA DSBs. We observed comet tails in both LNCaP *BRCA2*-gRNA2-cl7 and LNCaP *BRCA2*-gRNA 2 cells treated with dasatinib, whereas DMSO-treated cells did not have any significant comet tails (Supplementary Fig. S4A).

Dasatinib also induced DNA damage in RWPE1 cells, an immortalized benign human prostate cell line (Supplementary Fig. S4B). RWPE1 cells are *BRCA2* wild type (10) and express low levels of TP53 and RB1 proteins due to the presence of a single copy of human papillomavirus 18 (HPV18) (39). We also examined the effect of dasatinib on RWPE1 cell viability. Only the combination of olaparib and dasatinib significantly reduced cell viability; there was minimal decrease with dasatinib alone (Supplementary Fig. S4C). These data suggest that the combination of dasatinib and PARPi may inhibit the growth of PC cells without alterations in canonical DDR genes (e.g., BRCA2) but with alterations in tumor suppressors such as *TP53* or *RB1*. Taken together, our data show that inhibition of SRC signaling by dasatinib induces DNA damage in PC cells, thereby increasing sensitivity to PARPi.

We extend our study and investigated the effects of combined inhibition of SRC and PARP on the growth of *TP53*/*RB1*-null PC cells. Loss of *TP53* and *RB1* is observed in advanced PC and frequently observed in very aggressive neuroendocrine/neuroendocrine-like PC and is associated with poor outcome (8). To examine SRC activation in *TP53*/*RB1*-null neuroendocrine PC, we used localized prostate tumors from C57BL/6-Tg(TRAMP) mice; this genetically engineered mouse model expresses simian virus 40 (SV40) early genes (large and small tumor antigens, Tag) in the prostate, resulting in abrogation of *Trp53* and *Rb1* and the rapid development of androgen receptor–negative aggressive and metastatic neuroendocrine PC (40). We observed strong SRC phosphorylation and increased DNA damage (phosphorylation of γH2AX) in the Tg(TRAMP) tumors relative to the normal prostate of C57BL/6J mice (Fig. 4D). We treated TRAMP-C2 cells (tumorigenic cell lines developed from 32-week localized prostate of a Tg(TRAMP) mouse) (41) with dasatinib (0.3 μM) or bosutinib (0.3 μM) alone and in combination with talazoparib (0.03 μM) for 5 days. There was a significant reduction of cell viability when treatment included SRC inhibitors dasatinib or bosutinib in combination with talazoparib compared to treatment with either dasatinib, bosutinib, or talazoparib alone (Fig. 4E,F). We also treated TRAMP-C2 cells with 0.3 μM dasatinib and 0.1 μM cisplatin and observed a strong reduction in the viability of cells treated with the combination of dasatinib and cisplatin compared to treatment with either drug alone (Fig. 4G, Supplementary Fig. S4D). These data suggest that the combinatorial treatment of SRC inhibitors with PARPi or platinum-based chemotherapy strongly reduces viability over treatment with either SRC inhibitors or PARPi alone in *Trp53*/*Rb1*-null neuroendocrine PC.

We were unable to find any significant overlap between published SRC signaling genes and DDR genes (Supplementary Fig. S4E), indicating that further study to uncover the connection is warranted.

SRC activation may lead to PARPi resistance in PC

Although PARPi-based therapies are the mainstay for patients with *BRCA1/2*-mutated PC (14–16), responses are not durable; de novo and acquired PARPi resistance are major limiting factors of clinical therapy, though the mechanisms of resistance are not fully understood. We hypothesized that SRC activation is important in PARPi resistance in PC. We treated 22RV1 cells, which harbor a *BRCA2* oncogenic mutation (T3033Nfs*11) (42), with olaparib and dasatinib alone and in combination. Consistent with our previous report (10), 22RV1 cells had *de novo* relative resistance to olaparib (Fig. 5A). Combination treatment significantly decreased 22RV1 cell viability. Dasatinib alone had only a very modest effect.

We next performed a transient periodic experiment treating PC3M cells with dasatinib and talazoparib (Supplementary Fig. S5A). We first treated PC3M cells for 3 days with talazoparib or dasatinib alone. We then added dasatinib to the talazoparib pretreated cells (and vice versa) and incubated the cells for 4 days. Cells treated with talazoparib or dasatinib alone or in combination for 6 continuous days were used as control. Dasatinib considerably reduced the viability of talazoparib-pretreated cells (Fig. 5B, Supplementary Fig. S5A). There was a similar reduction of cell viability in dasatinib-pretreated cells in the presence of talazoparib (Fig. 5B, Supplementary Fig. S5A). As expected, combination treatment of dasatinib and talazoparib for 6 continuous days significantly reduced cell viability relative to either drug alone (Fig. 5B, Supplementary Fig. S5A). However, there was no significant difference in viability of cells pretreated or continuously treated with the talazoparib/dasatinib combination (Fig. 5B, Supplementary Fig. S5A).

We also incubated PC3M cells in olaparib- or talazoparib-supplemented media. After 15 days, we counted the surviving cell population (PARPi-resistant), replated, and treated with dasatinib with olaparib or talazoparib for 7 days (Supplementary Fig. S5B). Strikingly, the viability of PARPi-resistant cells was remarkably reduced in the presence of low concentrations of dasatinib (Fig. 5C,D). Dasatinib treatment only modestly reduced the viability of DMSO-pretreated cells (Fig. 5C,D). These data indicate that dasatinib restores PARPi sensitivity in PARPi-resistant PC cells.

We transiently knocked down *SRC* in PC3M cells and treated them with olaparib or talazoparib. PARPi selectively attenuated the viability of PC3M cells with decreased SRC expression (Fig. 5E). We next investigated whether SRC activation was directly involved in PARPi resistance in PC cells. We transiently overexpressed constitutively active SRC (Y527F SRC) (43) or empty vector in PC3M cells. Expression of constitutively active SRC rescued the cell viability reduction in response to PARPi (Fig. 5F). Collectively, these data further demonstrate that SRC activation may be a mechanism of PARPi resistance in PC.

Dasatinib and PARPi combination attenuates 3D PC organoid growth

Recent data have shown that 3D organoids are a better model for understanding disease biology and testing drug efficacy in vitro (44). We treated 3D Matrigel organoids of PC3M cells with dasatinib or olaparib alone or in combination (Supplementary Fig. S6A). Combination treatment remarkably reduced the number and size of organoid colonies compared to treatment with either drug alone (Fig. 6A,B). Treatment of LNCaP-abl organoids with dasatinib and talazoparib produced similar results (Fig. 6C, Supplementary Fig. S6B). We also observed reduced PC3M invasion through Matrigel in dasatinib-treated organoids compared to DMSO- or olaparib-treated organoids (Fig. 6B).

We extended our study to include organoids derived from patients with mCRPC, which can be used as avatars of human cancer to study the molecular mechanisms of candidate genes and the effect of drugs (29). We have previously used fluorescence in situ hybridization (FISH) to assess *BRCA2* status of these organoids; MSKPCa1 and MSKPCa3 have heterozygous loss of *BRCA2,* whereas MSKPCa2 is *BRCA2* wild type (10). All three patient-derived organoids exhibited high SRC activation compared to LNCaP cells (Fig. 6D). Interestingly, we observed high FAK phosphorylation only in the *BRCA2*-null organoids MSKPCa1 and MSKPCa3 but not in the *BRCA2* wild-type organoid MSKPCa2 (Fig. 6D). We treated the *BRCA2*-null organoids with 0.3 μM dasatinib and 0.03 μM talazoparib alone or in combination in 2D on collagen-coated plates or in 3D Matrigel. We observed a strong reduction in the viability of organoids in 2D culture (Fig. 6E) and a statistically significant reduction in the number of organoid colonies with combination treatment relative to treatment with either drug alone (Fig. 6F,G and Supplementary Fig. S6C). Our results suggest that combined inhibition of SRC and PARP could be more effective than targeting PARP alone in patients with *BRCA2*-altered tumors.

DISCUSSION

Recent studies have revealed germline and somatic variants in DDR pathway components in a significant subset of patients with PC (2,5,6). Studies have also shown that patients with mCRPC harbor germline mutations in DDR genes—including *BRCA2*—more frequently than those with localized disease (6,9). Patients with PC with germline *BRCA1/2* mutations were found to have more aggressive disease and poorer survival than patients with wild-type *BRCA1/2* (45). We have previously demonstrated that loss of even a single copy of *BRCA2* results in a worse prognosis in PC (10). In addition to its function as a guardian of genomic stability during replication stress and maintaining genomic integrity, *BRCA2* is a multifaceted tumor suppressor with numerous functions (46). Therefore, the discovery of the signaling pathways associated with *BRCA2* loss is crucial for identifying therapeutic targets.

DDR is a complex, multilevel process involving several sub-pathways (47). Generally, mutations/deficiencies in one component can be compensated for by other components/genes (48), which may be exploited to develop novel therapeutic strategies, such as using PARPi to treat cancers with DDR alterations (49). Studies have shown the benefits of combining PARPi with other therapies in cell lines and clinical trials (50). There was a synergistic reduction of apoptosis and DNA damage in multiple PC cell lines treated with the histone deacetylase inhibitor SAHA and the PARPi veliparib (51). Clinical trials

combining olaparib and checkpoint inhibitors and antiandrogen therapies have demonstrated efficacy in patients with DDR defects (52). A phase I/II trial with olaparib and cediranib, an angiogenesis inhibitor, in advanced solid tumors including mCRPC is ongoing (NCT02484404). This indicates that combination therapies with PARPi may be beneficial for patients with mCRPC—particularly those with DDR alterations.

We prospectively investigated the signaling pathways deregulated by *BRCA2* loss to identify novel therapeutic targets. We hypothesized that combining PARPi with inhibitors of activated signaling pathways would have a synergistic effect. We found that the SRC signaling pathway was activated in *BRCA2*-null mCRPC and increased SRC activation in *BRCA2*-null PC cell lines. We observed a synergistic reduction in cell viability in *BRCA2*-null PC cell lines—but not parental cells with wild-type *BRCA2*—treated with PARPi and dasatinib. We also showed that SRC activation may be involved in PARPi resistance in *BRCA2*-null PC cells. These data suggest the utility of combining dasatinib and PARPi in aggressive PC. We also found a remarkable reduction in the viability of *BRCA2*-null PC cells treated with dasatinib and cisplatin, indicating that dasatinib increases the efficacy of both PARPi and platinum-based chemotherapy.

Interestingly, we also observed that the combination of PARPi and SRC inhibitors resulted in a significant reduction in RWPE1 cell viability, even though this cell line has wild-type *BRCA2* and an intact canonical DDR pathway. However, RWPE1 cells express significantly lower RB1 and P53 protein due to their expression of a single copy of HPV 18 (39). We have also demonstrated that combination treatment with PARPi and SRC inhibitors reduces the growth of *Trp53*/*Rb1*-null androgen receptor–independent neuroendocrine PC. Our study is the first of its kind to combine SRC and PARP inhibition, and we hypothesize that this combination has great potential for patients harboring DDR alterations. We anticipate that this combination may also be effective in unselected patients without known DDR alterations whose tumors harbor alterations of classical tumor suppressors *RB1* and *p53*. However, this requires further testing to confirm the significance of the therapeutic combination beyond canonical DDR alterations.

SRC is a proto-oncogenic nonreceptor tyrosine kinase with roles in tumor cell proliferation, survival, and invasion (53). Inactivation of SRC signaling in response to DNA damage replication stress has been shown to suppress G1/S progression and maintain genomic stability (54), and induction of DNA damage has also been shown to induce SRC activation in breast cancer cells (55). We observed that inhibition of SRC by dasatinib induces defective DNA DSB repair. These data indicate that SRC activation is essential for DNA DSB repair and may be important in homologous recombination repair, which has not been previously reported. We also observed that *BRCA2* loss induces SRC-Y416 phosphorylation, suggesting that increased DSBs by *BRCA2* loss may activate SRC. Considering the complexity of the process, we believe that multiple mechanisms may also be involved in SRC-regulated DNA damage response.

SRC activation has been reported in several cancers, including PC (56). In a study that examined matched prostate tumor samples taken before hormone deprivation therapy and after relapse, 28% of castration-resistant tumors exhibited increased SRC activity (57).

Patients with high SRC activity had significantly shorter overall survival ($P < 0.0001$) (57). Induction of v-SRC alone is sufficient for oncogenic transformation of benign prostate cells and induces lung metastasis (58). SRC knockdown/inhibition reduces bone metastasis in a breast cancer xenograft model (59), and *SRC* knockdown inhibits the migration of PC cells in vitro (60). We observed that dasatinib suppresses elongated morphology of PC cells irrespective of *BRCA2* status and reduces invasion in 3D organoid culture, further indicating the association between SRC activation and invasive phenotype of cancer cells. Although alterations in the DDR pathway are far rarer in localized PC than in mCRPC (5), we did observe increased SRC activation (SRC Y416 phosphorylation) in a fraction of localized PC cases from TCGA cohort, which may be associated with aggressive disease and independent from *BRCA2* alteration status. Previous studies showed that activation of SRC induces androgen-independent growth of LNCaP cells and drives castration-resistant PC progression through an androgen receptor–dependent mechanism (61). These data indicate that activation of SRC may play an important role in primary PC progression and castration resistance, but further testing in a larger cohort and proteomic analyses are necessary to validate these findings.

Dasatinib (BMS-354825, Sprycel®) is a commercially available, multiple tyrosine kinase inhibitor that inhibits SRC activation. Although the role of SRC in tumor progression and metastasis is well established, dasatinib monotherapy has not shown significant promise in solid tumors (62). Dasatinib has been shown to inhibit cell adhesion, migration, and invasion of PC cell lines (63). Dasatinib inhibited tumor growth and the development of lymph node metastases in both castration-sensitive and castration-resistant tumors. It was also shown to decrease proliferation and increase apoptosis in orthotopic nude mouse models (60,62). Dasatinib suppressed disease progression in an intratibial xenograft model of PC3M cells (64). Mendiratta et al. reported that decreased predicted androgen receptor activity correlated with increased predicted SRC activity and sensitivity to dasatinib in androgen-sensitive LNCaP cells (65). Given these findings, dasatinib was evaluated in combination with docetaxel in the READY trial, a randomized phase III study of over 1500 unselected patients with mCRPC. There was no overall survival benefit in patients treated with docetaxel and dasatinib compared to docetaxel alone (66). However, dasatinib modestly prolonged time to skeletal events ($P = 0.08$, HR 0.81 [64–1.02]) (66). Similarly, previous preclinical observations showed that bosutinib and saracatinib also inhibited PC growth and metastasis in experimental mouse models (67,68). These findings demonstrate that identifying patients with high SRC activation is necessary to personalize SRC inhibitor–based therapy for patients with mCRPC.

Resistance to PARPi reduces drug efficacy and worsens patient outcomes (69). Because *BRCA2* is frequently deleted in PC, the mechanisms of resistance to PARPi in PC likely involve alternative molecular mechanisms rather than reversion mutation. We observed that the combination of dasatinib and olaparib greatly reduces the proliferation of 22RV1 cells, which harbor oncogenic mutation of *BRCA2* but exhibit resistance to PARPi. Moreover, the addition of dasatinib to PARPi in *BRCA2*-defective PC3M cells has enhanced the reduction in cell viability and may rescue secondary resistance developed during prior treatment with PARPi. We also observed that *SRC* knockdown increases the antiproliferative effect of PARPi, whereas overexpression of constitutively active SRC leads to relative resistance to

PARPi. Further study is needed to understand the molecular mechanism. Our data suggest that SRC activation may be a possible mechanism of PARPi resistance in PC; treatment with dasatinib, bosutinib, or saracatinib may overcome this resistance.

In conclusion, we identified high SRC activation in *BRCA2*-altered mCRPC. We found that the combined inhibition of SRC and PARP in *BRCA2*-altered PC cell lines and organoids had a synergistic effect on cell viability. For the first time, we demonstrated that SRC activation may be a potential mechanism of PARPi resistance and found that SRC inhibitors (e.g., dasatinib, bosutinib, saracatinib) may overcome this resistance. These results suggest that combination inhibition of PARP and SRC should be explored in men with *BRCA2*-mutated mCRPC.

Supplementary Material

Refer to Web version on PubMed Central for supplementary material.

Acknowledgements:

We thank Ralph Garippa, Hsiu Yu Liu, and staff of the MSK Gene Editing and Screening Core (formerly the RNAi Core) for CRISPR design and CRISPR sequencing, Yu Chen (MSK) for the organoids, Cindy Lee of the MSK Human Oncology and Pathogenesis Program for organoid culture media, Mesruh Turkekul of the MSK Molecular Cytology Core Facility for immunohistochemistry, and Sara DiNapoli and Amy Plofker (MSK) for editing.

Financial support: This work was supported by a Department of Defense Prostate Cancer Research Program award to PWK (W81XWH1910470), a Department of Defense Early Investigator Research Award (W81XWH-18-1-0330) to KHS, and Prostate Cancer Foundation Young Investigator Awards to GC, KHS, WA, and LAM. PWK and LAM were supported by a Prostate Cancer Foundation Challenge Award and by NCI grant 5P01CA228696-02. This work was supported in part by a grant from the National Institutes of Health to Memorial Sloan Kettering Cancer Center (P30CA008748).

Conflict of interest disclosure:

As of May 20, 2020, P.W. Kantoff reports the following disclosures for the last 24-month period: he has investment interest in Context Therapeutics LLC, DRGT, Placon, and Seer Biosciences; he is a company board member for Context Therapeutics LLC; he is a consultant/scientific advisory board member for Bavarian Nordic Immunotherapeutics, DRGT, GE Healthcare, Janssen, OncoCellMDX, Progenity, Seer Biosciences, and Tarveda Therapeutics; and he serves on data safety monitoring boards for Genentech/Roche and Merck.

W. Abida reports the following disclosures: he has received honoraria from CARET; he has a consulting/advisory role for Clovis Oncology, Janssen, MORE Health, Oric Pharmaceuticals, and Daiichi Sankyo; he has obtained research funding (institutional) from AstraZeneca, Clovis Oncology, GlaxoSmithKline, and Zenith Epigenetics; and he has received travel/accommodation expenses from Clovis Oncology, GlaxoSmithKline, and Oric Pharmaceuticals.

M. J. Morris reports the following disclosures: he is an uncompensated consultant for Endocyte, Advanced Accelerator Applications, and Johnson & Johnson; he is a compensated consultant for Curiur and ORIC; and he has obtained research funding (institutional, for clinical trial) from Bayer, Endocyte, Progenics, Corcept, Roche, and Janssen.

D. Danila reports the following disclosures: he has received research support from Janssen Research & Development, Astellas, Medivation, Agensys, Genentech, and CreaTV; he is a consultant for Angle LLT, Janssen Research & Development, Astellas, Agensys, and Medivation.

REFERENCES

1. Dong L, Zieren RC, Xue W, de Reijke TM, Pienta KJ. Metastatic prostate cancer remains incurable, why? Asian J Urol 2019;6(1):26–41. doi 10.1016/j.ajur.2018.11.005. [PubMed: 30775246]

2. Robinson D, Van Allen EM, Wu YM, Schultz N, Lonigro RJ, Mosquera JM, et al. Integrative clinical genomics of advanced prostate cancer. Cell 2015;161(5):1215–28. doi 10.1016/j.cell.2015.05.001. [PubMed: 26000489]

3. Abida W, Cyrta J, Heller G, Prandi D, Armenia J, Coleman I, et al. Genomic correlates of clinical outcome in advanced prostate cancer. Proc Natl Acad Sci U S A 2019;116(23):11428–36. doi 10.1073/pnas.1902651116. [PubMed: 31061129]

4. Jeggo PA, Pearl LH, Carr AM. DNA repair, genome stability and cancer: a historical perspective. Nat Rev Cancer 2016;16(1):35–42. doi 10.1038/nrc.2015.4. [PubMed: 26667849]

5. Armenia J, Wankowicz SAM, Liu D, Gao J, Kundra R, Reznik E, et al. The long tail of oncogenic drivers in prostate cancer. Nat Genet 2018;50(5):645–51. doi 10.1038/s41588-018-0078-z. [PubMed: 29610475]

6. Pritchard CC, Mateo J, Walsh MF, De Sarkar N, Abida W, Beltran H, et al. Inherited DNA-repair gene mutations in men with metastatic prostate cancer. N Engl J Med 2016;375(5):443–53. doi 10.1056/NEJMoa1603144. [PubMed: 27433846]

7. Arce S, Athie A, Pritchard CC, Mateo J. Germline and somatic defects in DNA repair pathways in prostate cancer. Adv Exp Med Biol 2019;1210:279–300. doi 10.1007/978-3-030-32656-2_12. [PubMed: 31900913]

8. Beltran H, Romanel A, Conteduca V, Casiraghi N, Sigouros M, Franceschini GM, et al. Circulating tumor DNA profile recognizes transformation to castration-resistant neuroendocrine prostate cancer. J Clin Invest 2020;130(4):1653–68. doi 10.1172/JCI131041. [PubMed: 32091413]

9. Castro E, Romero-Laorden N, Del Pozo A, Lozano R, Medina A, Puente J, et al. PROREPAIR-B: a prospective cohort study of the impact of germline DNA repair mutations on the outcomes of patients with metastatic castration-resistant prostate cancer. J Clin Oncol 2019;37(6):490–503. doi 10.1200/JCO.18.00358. [PubMed: 30625039]

10. Chakraborty G, Armenia J, Mazzu YZ, Nandakumar S, Stopsack KH, Atiq MO, et al. Significance of BRCA2 and RB1 co-loss in aggressive prostate cancer progression. Clin Cancer Res 2020;26(8):2047–64. doi 10.1158/1078-0432.CCR-19-1570. [PubMed: 31796516]

11. Chang HHY, Pannunzio NR, Adachi N, Lieber MR. Non-homologous DNA end joining and alternative pathways to double-strand break repair. Nat Rev Mol Cell Biol 2017;18(8):495–506. doi 10.1038/nrm.2017.48. [PubMed: 28512351]

12. Lord CJ, Ashworth A. PARP inhibitors: synthetic lethality in the clinic. Science 2017;355(6330):1152–8. doi 10.1126/science.aam7344. [PubMed: 28302823]

13. Mateo J, Lord CJ, Serra V, Tutt A, Balmana J, Castroviejo-Bermejo M, et al. A decade of clinical development of PARP inhibitors in perspective. Ann Oncol 2019;30(9):1437–47. doi 10.1093/annonc/mdz192. [PubMed: 31218365]

14. Mateo J, Carreira S, Sandhu S, Miranda S, Mossop H, Perez-Lopez R, et al. DNA-repair defects and olaparib in metastatic prostate cancer. N Engl J Med 2015;373(18):1697–708. doi 10.1056/NEJMoa1506859. [PubMed: 26510020]

15. Abida W, Campbell D, Patnaik A, Shapiro JD, Sautois B, Vogelzang NJ, et al. Non-BRCA DNA damage repair gene alterations and response to the PARP inhibitor rucaparib in metastatic castration-resistant prostate cancer: analysis from the phase II TRITON2 study. Clin Cancer Res 2020;26(11):2487–96. doi 10.1158/1078-0432.CCR-20-0394. [PubMed: 32086346]

16. de Bono J, Mateo J, Fizazi K, Saad F, Shore N, Sandhu S, et al. Olaparib for metastatic castration-resistant prostate cancer. N Engl J Med 2020;382:2091–2102. doi 10.1056/NEJMoa1911440. [PubMed: 32343890]

17. Food and Drug Administration [press release, May 15, 2020]. FDA grants accelerated approval to rucaparib for BRCA-mutated metastatic castration-resistant prostate cancer. https://www.fda.gov/drugs/fda-grants-accelerated-approval-rucaparib-brca-mutated-metastatic-castration-resistant-prostate.

18. Food and Drug Administration [press release, May 20, 2020]. FDA approves olaparib for HRR gene-mutated metastatic castration-resistant prostate cancer. https://www.fda.gov/drugs/drug-approvals-and-databases/fda-approves-olaparib-hrr-gene-mutated-metastatic-castration-resistant-prostate-cancer.

19. Jonsson P, Bandlamudi C, Cheng ML, Srinivasan P, Chavan SS, Friedman ND, et al. Tumour lineage shapes BRCA-mediated phenotypes. Nature 2019;571(7766):576–9. doi 10.1038/s41586-019-1382-1. [PubMed: 31292550]
20. Pan ZY, Liang J, Zhang QA, Lin JR, Zheng ZZ. In vivo reflectance confocal microscopy of extramammary Paget disease: diagnostic evaluation and surgical management. J Am Acad Dermatol 2012;66(2):e47–53. doi 10.1016/j.jaad.2010.09.722. [PubMed: 21620517]
21. D'Andrea AD. Mechanisms of PARP inhibitor sensitivity and resistance. DNA Repair (Amst) 2018;71:172–6. doi 10.1016/j.dnarep.2018.08.021. [PubMed: 30177437]
22. Vlaeminck-Guillem V, Gillet G, Rimokh R. SRC: marker or actor in prostate cancer aggressiveness. Front Oncol 2014;4:222. doi 10.3389/fonc.2014.00222. [PubMed: 25184116]
23. Drake JM, Paull EO, Graham NA, Lee JK, Smith BA, Titz B, et al. Phosphoproteome integration reveals patient-specific networks in prostate cancer. Cell 2016;166(4):1041–54. doi 10.1016/j.cell.2016.07.007. [PubMed: 27499020]
24. Gelman IH, Peresie J, Eng KH, Foster BA. Differential requirement for Src family tyrosine kinases in the initiation, progression, and metastasis of prostate cancer. Mol Cancer Res 2014;12(10):1470–9. doi 10.1158/1541-7786.MCR-13-0490-T. [PubMed: 25053806]
25. Fukumoto Y, Morii M, Miura T, Kubota S, Ishibashi K, Honda T, et al. Src family kinases promote silencing of ATR-Chk1 signaling in termination of DNA damage checkpoint. J Biol Chem 2014;289(18):12313–29. doi 10.1074/jbc.M113.533752. [PubMed: 24634213]
26. Miura T, Fukumoto Y, Morii M, Honda T, Yamaguchi N, Nakayama Y, et al. Src family kinases maintain the balance between replication stress and the replication checkpoint. Cell Biol Int 2016;40(1):16–26. doi 10.1002/cbin.10517. [PubMed: 26194897]
27. Cerami E, Gao J, Dogrusoz U, Gross BE, Sumer SO, Aksoy BA, et al. The cBio cancer genomics portal: an open platform for exploring multidimensional cancer genomics data. Cancer Discov 2012;2(5):401–4. doi 10.1158/2159-8290.CD-12-0095. [PubMed: 22588877]
28. Gao J, Aksoy BA, Dogrusoz U, Dresdner G, Gross B, Sumer SO, et al. Integrative analysis of complex cancer genomics and clinical profiles using the cBioPortal. Sci Signal 2013;6(269):pl1. doi 10.1126/scisignal.2004088.
29. Gao D, Vela I, Sboner A, Iaquinta PJ, Karthaus WR, Gopalan A, et al. Organoid cultures derived from patients with advanced prostate cancer. Cell 2014;159(1):176–87. doi 10.1016/j.cell.2014.08.016. [PubMed: 25201530]
30. Chou TC. Drug combination studies and their synergy quantification using the Chou-Talalay method. Cancer Res 2010;70(2):440–6. doi 10.1158/0008-5472.CAN-09-1947. [PubMed: 20068163]
31. Gao H, Chakraborty G, Zhang Z, Akalay I, Gadiya M, Gao Y, et al. Multi-organ site metastatic reactivation mediated by non-canonical discoidin domain receptor 1 signaling. Cell 2016;166(1):47–62. doi 10.1016/j.cell.2016.06.009. [PubMed: 27368100]
32. Kumar A, Coleman I, Morrissey C, Zhang X, True LD, Gulati R, et al. Substantial interindividual and limited intraindividual genomic diversity among tumors from men with metastatic prostate cancer. Nat Med 2016;22(4):369–78. doi 10.1038/nm.4053. [PubMed: 26928463]
33. Chen J, Bardes EE, Aronow BJ, Jegga AG. ToppGene Suite for gene list enrichment analysis and candidate gene prioritization. Nucleic Acids Res 2009;37(Web Server issue):W305–11. doi 10.1093/nar/gkp427. [PubMed: 19465376]
34. Harvey R, Hehir KM, Smith AE, Cheng SH. pp60c-src variants containing lesions that affect phosphorylation at tyrosines 416 and 527. Mol Cell Biol 1989;9(9):3647–56. doi 10.1128/mcb.9.9.3647. [PubMed: 2476663]
35. Westhoff MA, Serrels B, Fincham VJ, Frame MC, Carragher NO. SRC-mediated phosphorylation of focal adhesion kinase couples actin and adhesion dynamics to survival signaling. Mol Cell Biol 2004;24(18):8113–33. doi 10.1128/MCB.24.18.8113-8133.2004. [PubMed: 15340073]
36. Selvaraj SK, Giri RK, Perelman N, Johnson C, Malik P, Kalra VK. Mechanism of monocyte activation and expression of proinflammatory cytochemokines by placenta growth factor. Blood 2003;102(4):1515–24. doi 10.1182/blood-2002-11-3423. [PubMed: 12689930]
37. Kim KJ, Cho CS, Kim WU. Role of placenta growth factor in cancer and inflammation. Exp Mol Med 2012;44(1):10–19. doi 10.3858/emm.2012.44.1.023. [PubMed: 22217448]

38. Mota JM, Barnett E, Nauseef JT, Nguyen B, Stopsack KH, Wibmer A, et al. Platinum-based chemotherapy in metastatic prostate cancer with DNA repair gene alterations. JCO Precis Oncol 2020;4:355–66. doi 10.1200/po.19.00346. [PubMed: 32856010]
39. Bello D, Webber MM, Kleinman HK, Wartinger DD, Rhim JS. Androgen responsive adult human prostatic epithelial cell lines immortalized by human papillomavirus 18. Carcinogenesis 1997;18(6):1215–23. doi 10.1093/carcin/18.6.1215. [PubMed: 9214605]
40. Bianchi-Frias D, Hernandez SA, Coleman R, Wu H, Nelson PS. The landscape of somatic chromosomal copy number aberrations in GEM models of prostate carcinoma. Mol Cancer Res 2015;13(2):339–47. doi 10.1158/1541-7786.MCR-14-0262. [PubMed: 25298407]
41. Foster BA, Gingrich JR, Kwon ED, Madias C, Greenberg NM. Characterization of prostatic epithelial cell lines derived from transgenic adenocarcinoma of the mouse prostate (TRAMP) model. Cancer Res 1997;57(16):3325–30. [PubMed: 9269988]
42. Barretina J, Caponigro G, Stransky N, Venkatesan K, Margolin AA, Kim S, et al. The Cancer Cell Line Encyclopedia enables predictive modelling of anticancer drug sensitivity. Nature 2012;483(7391):603–7. doi 10.1038/nature11003. [PubMed: 22460905]
43. Patwardhan P, Resh MD. Myristoylation and membrane binding regulate c-Src stability and kinase activity. Mol Cell Biol 2010;30(17):4094–107. doi 10.1128/MCB.00246-10. [PubMed: 20584982]
44. Drost J, Clevers H. Organoids in cancer research. Nat Rev Cancer 2018;18(7):407–18. doi 10.1038/s41568-018-0007-6. [PubMed: 29692415]
45. Castro E, Goh C, Olmos D, Saunders E, Leongamornlert D, Tymrakiewicz M, et al. Germline BRCA mutations are associated with higher risk of nodal involvement, distant metastasis, and poor survival outcomes in prostate cancer. J Clin Oncol 2013;31(14):1748–57. doi 10.1200/JCO.2012.43.1882. [PubMed: 23569316]
46. Martinez JS, Baldeyron C, Carreira A. Molding BRCA2 function through its interacting partners. Cell Cycle 2015;14(21):3389–95. doi 10.1080/15384101.2015.1093702. [PubMed: 26566862]
47. Hoeijmakers JH. Genome maintenance mechanisms for preventing cancer. Nature 2001;411(6835):366–74. doi 10.1038/35077232. [PubMed: 11357144]
48. Knijnenburg TA, Wang L, Zimmermann MT, Chambwe N, Gao GF, Cherniack AD, et al. Genomic and molecular landscape of DNA damage repair deficiency across The Cancer Genome Atlas. Cell Rep 2018;23(1):239–54.e6. doi 10.1016/j.celrep.2018.03.076. [PubMed: 29617664]
49. Dietlein F, Thelen L, Reinhardt HC. Cancer-specific defects in DNA repair pathways as targets for personalized therapeutic approaches. Trends Genet 2014;30(8):326–39. doi 10.1016/j.tig.2014.06.003. [PubMed: 25017190]
50. Pezaro C PARP inhibitor combinations in prostate cancer. Ther Adv Med Oncol 2020;12:1758835919897537. doi 10.1177/1758835919897537.
51. Yin L, Liu Y, Peng Y, Peng Y, Yu X, Gao Y, et al. PARP inhibitor veliparib and HDAC inhibitor SAHA synergistically co-target the UHRF1/BRCA1 DNA damage repair complex in prostate cancer cells. J Exp Clin Cancer Res 2018;37(1):153. doi 10.1186/s13046-018-0810-7. [PubMed: 30012171]
52. Lee JM, Cimino-Mathews A, Peer CJ, Zimmer A, Lipkowitz S, Annunziata CM, et al. Safety and clinical activity of the programmed death-ligand 1 inhibitor durvalumab in combination with poly (ADP-ribose) polymerase inhibitor olaparib or vascular endothelial growth factor receptor 1–3 inhibitor cediranib in women's cancers: a dose-escalation, phase I study. J Clin Oncol 2017;35(19):2193–202. doi 10.1200/JCO.2016.72.1340. [PubMed: 28471727]
53. Sen B, Johnson FM. Regulation of SRC family kinases in human cancers. J Signal Transduct 2011;2011:865819. doi 10.1155/2011/865819. [PubMed: 21776389]
54. Shields BJ, Hauser C, Bukczynska PE, Court NW, Tiganis T. DNA replication stalling attenuates tyrosine kinase signaling to suppress S phase progression. Cancer Cell 2008;14(2):166–79. doi 10.1016/j.ccr.2008.06.003. [PubMed: 18691551]
55. Li Z, Hosoi Y, Cai K, Tanno Y, Matsumoto Y, Enomoto A, et al. Src tyrosine kinase inhibitor PP2 suppresses ERK1/2 activation and epidermal growth factor receptor transactivation by X-irradiation. Biochem Biophys Res Commun 2006;341(2):363–8. doi 10.1016/j.bbrc.2005.12.193. [PubMed: 16414009]

56. Drake JM, Graham NA, Stoyanova T, Sedghi A, Goldstein AS, Cai H, et al. Oncogene-specific activation of tyrosine kinase networks during prostate cancer progression. Proc Natl Acad Sci U S A 2012;109(5):1643–8. doi 10.1073/pnas.1120985109. [PubMed: 22307624]
57. Tatarov O, Mitchell TJ, Seywright M, Leung HY, Brunton VG, Edwards J. SRC family kinase activity is up-regulated in hormone-refractory prostate cancer. Clin Cancer Res 2009;15(10):3540–9. doi 10.1158/1078-0432.CCR-08-1857. [PubMed: 19447874]
58. Ju X, Ertel A, Casimiro MC, Yu Z, Meng H, McCue PA, et al. Novel oncogene-induced metastatic prostate cancer cell lines define human prostate cancer progression signatures. Cancer Res 2013;73(2):978–89. doi 10.1158/0008-5472.CAN-12-2133. [PubMed: 23204233]
59. Zhang XH, Wang Q, Gerald W, Hudis CA, Norton L, Smid M, et al. Latent bone metastasis in breast cancer tied to Src-dependent survival signals. Cancer Cell 2009;16(1):67–78. doi 10.1016/j.ccr.2009.05.017. [PubMed: 19573813]
60. Saad F Src as a therapeutic target in men with prostate cancer and bone metastases. BJU Int 2009;103(4):434–40. doi 10.1111/j.1464-410X.2008.08249.x. [PubMed: 19154462]
61. Chattopadhyay I, Wang J, Qin M, Gao L, Holtz R, Vessella RL, et al. Src promotes castration-recurrent prostate cancer through androgen receptor-dependent canonical and non-canonical transcriptional signatures. Oncotarget 2017;8(6):10324–47. doi 10.18632/oncotarget.14401. [PubMed: 28055971]
62. Zhang S, Yu D. Targeting Src family kinases in anti-cancer therapies: turning promise into triumph. Trends Pharmacol Sci 2012;33(3):122–8. doi 10.1016/j.tips.2011.11.002. [PubMed: 22153719]
63. Nam S, Kim D, Cheng JQ, Zhang S, Lee JH, Buettner R, et al. Action of the Src family kinase inhibitor, dasatinib (BMS-354825), on human prostate cancer cells. Cancer Res 2005;65(20):9185–9. doi 10.1158/0008-5472.CAN-05-1731. [PubMed: 16230377]
64. Yano A, Tsutsumi S, Soga S, Lee MJ, Trepel J, Osada H, et al. Inhibition of Hsp90 activates osteoclast c-Src signaling and promotes growth of prostate carcinoma cells in bone. Proc Natl Acad Sci U S A 2008;105(40):15541–6. doi 10.1073/pnas.0805354105. [PubMed: 18840695]
65. Mendiratta P, Mostaghel E, Guinney J, Tewari AK, Porrello A, Barry WT, et al. Genomic strategy for targeting therapy in castration-resistant prostate cancer. J Clin Oncol 2009;27(12):2022–9. doi 10.1200/JCO.2008.17.2882. [PubMed: 19289629]
66. Araujo JC, Trudel GC, Saad F, Armstrong AJ, Yu EY, Bellmunt J, et al. Docetaxel and dasatinib or placebo in men with metastatic castration-resistant prostate cancer (READY): a randomised, double-blind phase 3 trial. Lancet Oncol 2013;14(13):1307–16. doi 10.1016/S1470-2045(13)70479-0. [PubMed: 24211163]
67. Rabbani SA, Valentino ML, Arakelian A, Ali S, Boschelli F. SKI-606 (bosutinib) blocks prostate cancer invasion, growth, and metastasis in vitro and in vivo through regulation of genes involved in cancer growth and skeletal metastasis. Mol Cancer Ther 2010;9(5):1147–57. doi 10.1158/1535-7163.MCT-09-0962. [PubMed: 20423991]
68. Yang JC, Bai L, Yap S, Gao AC, Kung HJ, Evans CP. Effect of the specific Src family kinase inhibitor saracatinib on osteolytic lesions using the PC-3 bone model. Mol Cancer Ther 2010;9(6):1629–37. doi 10.1158/1535-7163.MCT-09-1058. [PubMed: 20484016]
69. Pettitt SJ, Lord CJ. Dissecting PARP inhibitor resistance with functional genomics. Curr Opin Genet Dev 2019;54:55–63. doi 10.1016/j.gde.2019.03.001. [PubMed: 30954761]

Statement of Translational Relevance

PARP inhibitors are promising for men with metastatic castration-resistant prostate cancer (mCRPC) who harbor defects in the DNA damage repair pathway, but the effects are not durable. Additional therapeutic approaches are needed in order to leverage and improve upon the clinical benefits of PARP inhibitors. We found that the oncogenic SRC signaling pathway was activated in *BRCA2*-altered mCRPC, and experimentally we showed that SRC phosphorylation was increased in CRISPR-mediated *BRCA2*-knockout human prostate cancer cell lines. Dual inhibition of PARP and SRC had a synergistic inhibitory effect on the growth of *BRCA2*-null prostate cancer cell lines, patient-derived organoids, and Trp53/Rb1-null prostate cancer cells. We also showed that activation of SRC may induce PARP inhibitor resistance in *BRCA2*-null prostate cancer cells. For the first time, our data demonstrate that combined inhibition of SRC and PARP can overcome PARP inhibitor resistance, suggesting that this drug combination should be investigated through clinical trials.

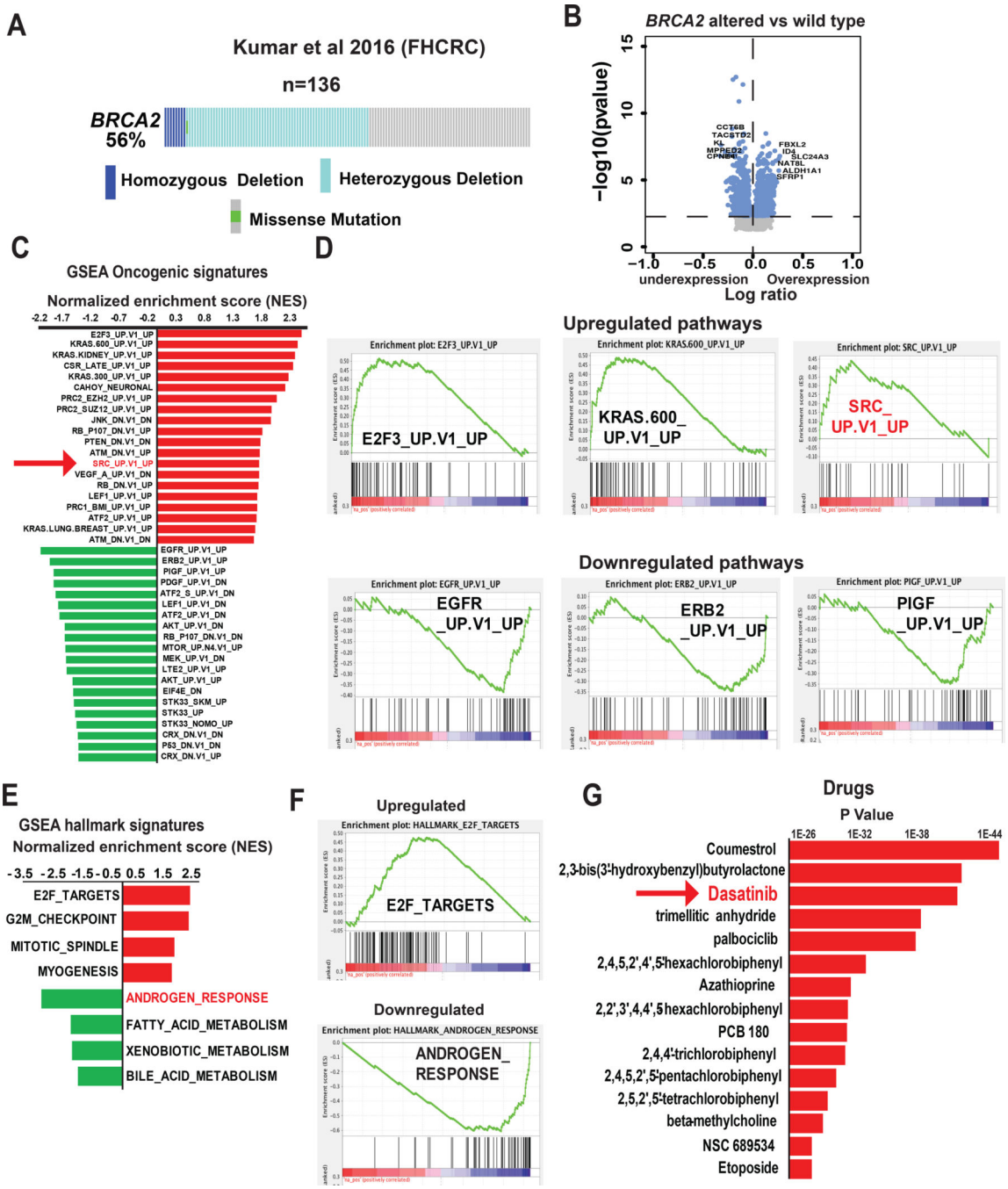

Figure 1. Activation of SRC signaling pathway in *BRCA2*-deleted prostate cancer

(A) *BRCA2* alteration status of samples in the Kumar et al. 2016 metastatic castration-resistant prostate cancer (mCRPC) cohort. Data from patients with complete mutation and copy number alteration (CNA) information were analyzed (134 samples from 54 patients). **(B)** Volcano plot shows genes that are altered in *BRCA2*-deleted (homozygous + heterozygous) compared to samples with wild-type *BRCA2*. **(C)** The bar graph shows the oncogenic pathways that are altered in *BRCA2*-deleted (homozygous + heterozygous) mCRPC tumors in Kumar et al. cohort. Pathway analyses were performed using GSEA (c6

oncogenic signature). The 20 most upregulated and downregulated (based on normalized enrichment score [NES]) pathways are shown. **(D)** Enrichment plots show the represented oncogenic pathways including upregulation of SRC oncogenic signatures (NES = 1.78, P = 0.003, Q = 0.05). **(E, F)** The bar graph and enrichment plots represent the hallmark signaling pathways that are significantly altered in *BRCA2*-deleted (homozygous + heterozygous) mCRPC tumors in the Kumar et al. cohort. Pathway analyses were performed using gene set enrichment analysis (GSEA) (Hallmark signature). **(G)** The bar graph shows the drugs which are significantly associated with the genes that are upregulated in *BRCA2*-deleted mCRPC described in Fig 1B. The gene-drug association analysis was performed using Toppgene Suite.

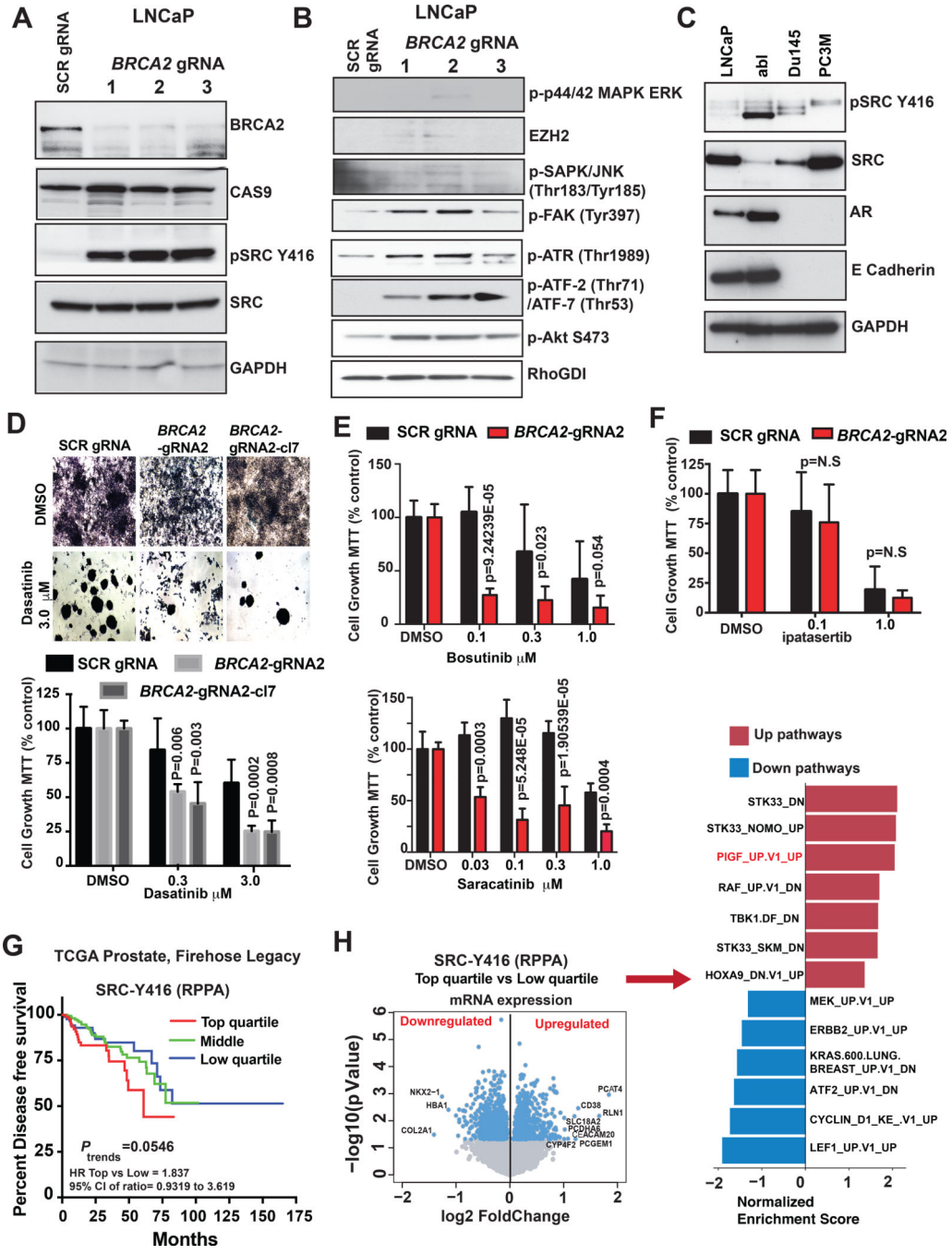

Figure 2. *BRCA2* deletion induces SRC kinase activation and increases sensitivity of prostate cancer cells to dasatinib

(A&B) LNCaP cells were transduced with three different guide RNAs (gRNAs) targeting *BRCA2*. Cells infected with scrambled (SCR) gRNA were used as control. CAS9, total SRC, GAPDH and RhoGDI served as loading controls. **(C)** Levels of phosphorylated SRC at tyrosine 416 (pSRC Y416), total SRC, androgen receptor (AR), and E-cadherin were assessed by western blot in prostate cancer cell lines. GAPDH was used as loading control. **(D)** Cells were treated with 0.3 and 3.0 μM dasatinib for 7 days. The equivalent volume of

DMSO was used as placebo treatment. After 7 days cells were treated with 0.5 mg/mL MTT and micrographed in 40x magnification (top). The bar graph shows the changes in cell growth percentage compared to scrambled (SCR) gRNA and DMSO treated samples (bottom). *P* values were calculated by Student t-test. **(E)** LNCaP SCR control and *BRCA2*-gRNA 2 cells were counted and plated in 96-well plates (2500 cells/well in 100 μL media). Cells were treated with Indicated concentration of bosutinib (top) or saracatinib (bottom) for 7 days. The equivalent volume of DMSO was used as a placebo treatment. Cells were treated with 0.5 mg/mL MTT and the graphs represent cell viability (MTT count, % control). *P* values were calculated by Student t-test. **(F)** Indicated cells (LNCaP SCR control and *BRCA2*-gRNA 2) were counted and plated in 96-well plates (2500 cells/well in 100 μL media) and treated with 0.1 and 1.0 μM concentration of ipatasertib for 7 days. The equivalent volume of DMSO was used as a placebo treatment. Cells were treated with 0.5 mg/mL MTT, measured in a plate reader at 570 nM and represented in the form of a bar graph. *P* values were calculated by Student t-test. **(G)** Samples from patients in The Cancer Genome Atlas (TCGA) Firehose Legacy cohort were divided into 4 quartiles based on levels of phospho-SRC at Y416, reverse-phase protein arrays (RPPA). Kaplan-Meier curves were used to compare disease-free survival. Log-rank test was performed to examine significance. **(H)** Volcano plot shows genes that are altered in phospho-SRC Y416 high (upper quartile RPPA value) cases compared to samples with phospho-SRC Y416 low (lower quartile RPPA value). The bar graph to the right of the volcano plot shows the oncogenic pathways that are altered in phospho-SRC Y416 high vs low localized PC tumors of The Cancer Genome Atlas (TCGA) Firehose Legacy cohort. Pathway analyses were performed using GSEA (c6 oncogenic signature). The altered (based on normalized enrichment score [NES]) pathways are shown.

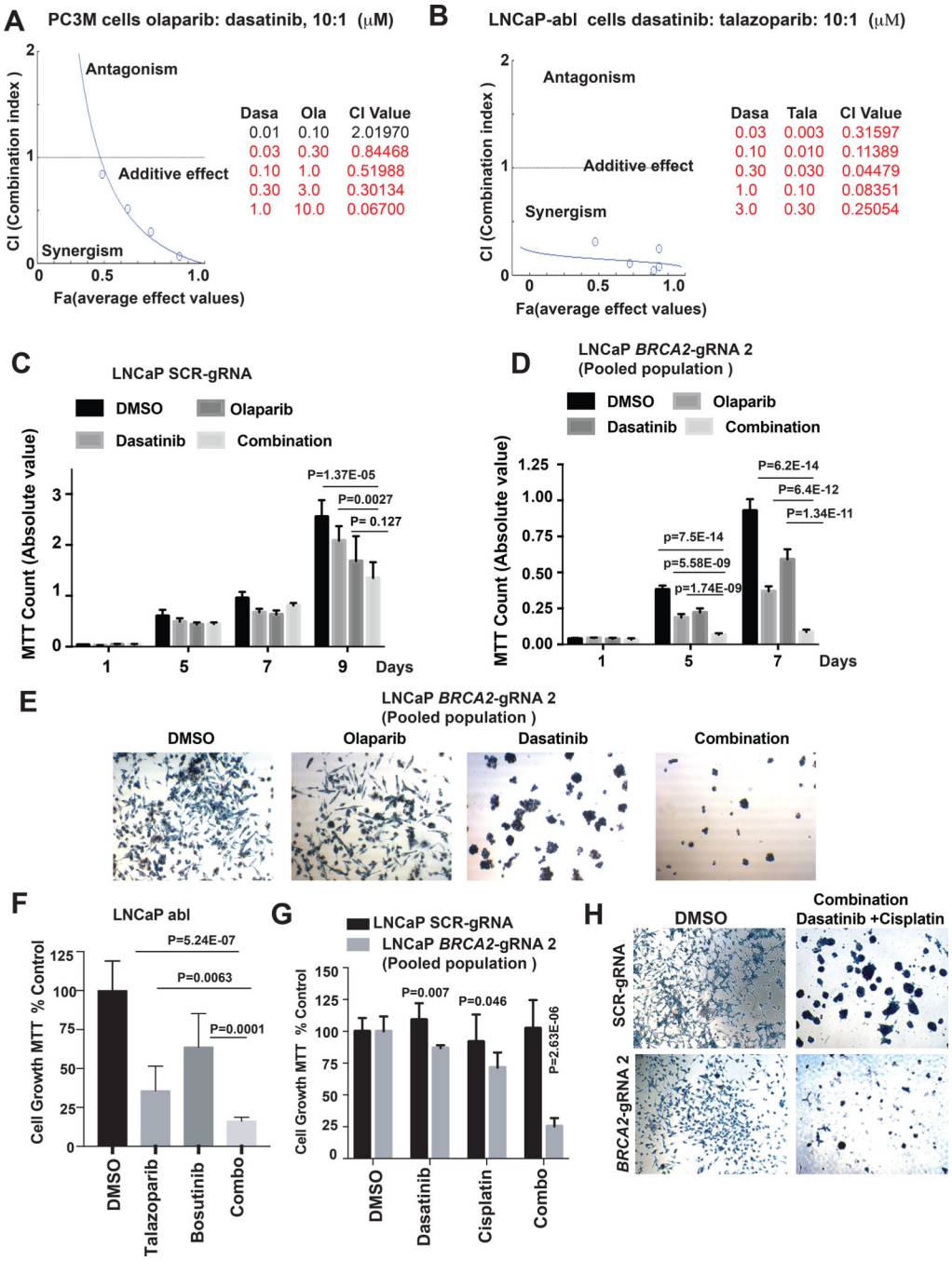

Figure 3. Synergistic effect of dasatinib and PARPi on *BRCA2*-null prostate cancer cell viability

(A,B) PC3M and LNCaP-abl cells were treated with indicated drugs alone or in combination for 4 days. Drug synergy was calculated using Chou-Talay Method/Compusyn. Left, graphs show the combination index (CI) plot for dasatinib with olaparib/talazoparib combination obtained from Compusyn. Right, tables show dose-dependent CI and average effect (Fa) values. **(C,D)** LNCaP SCR controls and *BRCA2*-gRNA 2 cells were counted and plated in 96-well plates (2500 cells/well in 100 μL media). Cells were treated with dasatinib (0.3 μM) and olaparib (3 μM) alone or in combination. The equivalent volume of DMSO was used as

a placebo treatment. After indicated days, cells were treated with 0.5 mg/mL MTT. The graphs represent the inhibition of cell viability by combination treatment. *P* values were calculated by Student t-test. **(E)** MTT-treated LNCaP-*BRCA2*-gRNA 2 cells from D were photographed at 40X magnification. Representative images are shown. **(F)** LNCaP abl cells were counted and plated in 96-well plates (2500 cells/well in 100 μL media). Cells were treated with bosutinib (0.3 μM) and talazoparib (0.03 μM) alone or in combination. The equivalent volume of DMSO was used as a placebo treatment. After 7 days, cells were treated with 0.5 mg/mL MTT, measured in a plate reader at 570 nM, and represented as a bar graph. **(G)** LNCaP SCR controls and *BRCA2*-gRNA 2 cells were counted and plated in 96-well plates (2500 cells/well in 100 μL media). Cells were treated with dasatinib (0.3 μM) and cisplatin (0.1 μM; dissolved in DMSF) alone or in combination. The equivalent volume of DMSO was used as a placebo treatment. After the indicated number of days, cells were treated with 0.5 mg/mL MTT. The graph represents the inhibition of cell viability by single and combination treatment. *P* values were calculated by Student t-test. **(H)** MTT-treated cells from G (DMSO and combination treatment) were photographed at 40X magnification. Representative images are shown.

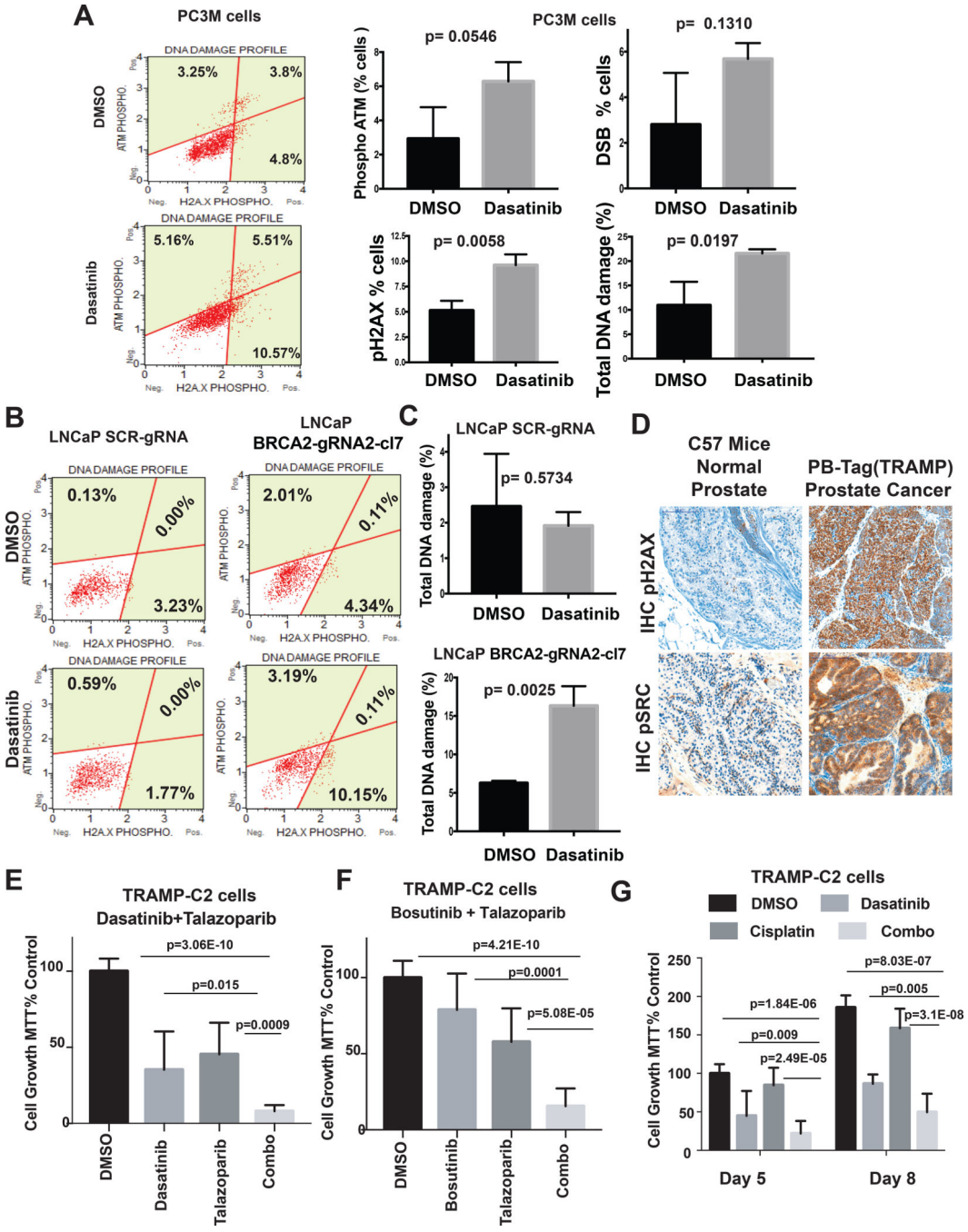

Figure 4. Dasatinib induces DNA damage in *BRCA2* null prostate cancer cells

(A) PC3M cells treated with dasatinib (0.3 μM) for 24 hours. The equivalent volume of DMSO was used as a placebo treatment. Left, dot plots show the percentage of cells with phospho-ATM, phospho-H2A.X, and both phospho-ATM and phospho-H2A.X. Right, bar graphs compare the percentages of cells between DMSO- and dasatinib-treated conditions (± SD). DSB (double-strand break) represents the percentage of cells with dual activation of ATM and H2A.X. Total DNA damage represents the percentage of cells with either activated ATM, activated H2A.X, or dual activation. *P* values were calculated by Student t-test. **(B**

&C) LNCaP SCR-gRNA and *BRCA2*-gRNA2 cl7 cells were treated with dasatinib (0.3 μM) for 24 hours. The equivalent volume of DMSO was used as a placebo treatment. Left, dot plots show the percentage of cells with phospho-ATM, phospho-H2A.X, and both phospho-ATM and phospho-H2A.X. Right, total DNA damage represents the percentage of cells with either activated ATM, activated H2A.X, or dual activation. *P* values were calculated by Student t-test. **(D)** Representative immunohistochemistry (IHC) images of paraffin-embedded sections of normal prostate from wild-type C57BL/6J mice and localized prostate tumors from PB-Tag mice. Sections were stained immunohistochemically with indicated antibodies (Brown). Nuclei were co-stained with hematoxylin (blue). The micrographs were captured in 200x magnification. Note that prostate tumors of PB-Tag mice exhibit higher DNA damage (increased phosphorylation of γH2AX) and Src activation (Src y416 phosphorylation) compared to normal mice prostate. **(E &F)** TRAMP-C2 cells (2500 cells/well in 100 μL media) were treated with dasatinib/bosutinib (0.3 μM) and talazoparib (0.03 μM) alone or in combination for 7 days. DMSO was used as a placebo treatment. Cell viability (± SD) was measured by MTT assay. **(G)** TRAMP-C2 cells were treated with dasatinib (0.3 μM) and cisplatin (0.1 μM; dissolved in DMSF) alone or in combination for 5 and 8 days. The equivalent volume of DMSO was used as a placebo treatment. After indicated number of days, cells were treated with 0.5 mg/mL MTT. The graphs represent the inhibition of cell viability by single and combination treatment. *P* values were calculated by Student t-test.

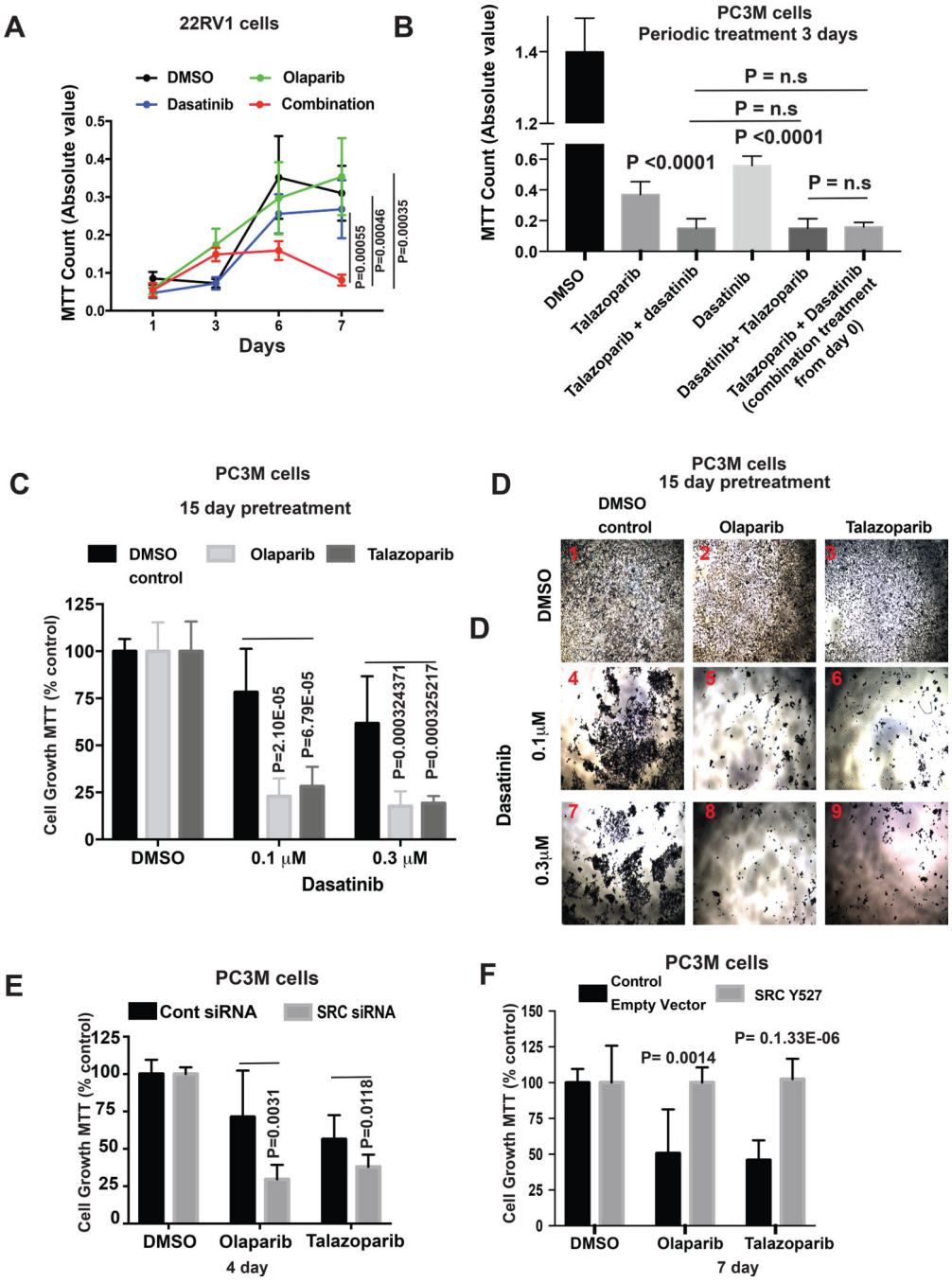

Figure 5. SRC activation leads to PARPi resistance

A) Viability (± SD) of 22RV1 cells treated with dasatinib (0.3 μM) ± olaparib (3.0 μM) as assessed by MTT assay. DMSO was used as a placebo control. (**B**) Viability (± SD) of PC3M cells subject to periodic treatment with talazoparib followed by dasatinib or vice versa, as assessed by MTT assay. DMSO was used as a placebo control. See Supplementary Fig. S5A for experimental schematic. *P* values were calculated by Student t-test. **(C&D)** PC3M cells were incubated in either olaparib (3.0 μM) or talazoparib (0.03 μM) supplemented media for 15 days to develop partial PARPi resistance. PARPi-resistant cells

were counted and treated with dasatinib (see Supplementary Fig. S5B for experimental schematic). Cell viability was assessed by MTT assay. Viability (± SD) of PC3M cells after 7 days of dasatinib treatment is shown in C. Representative images of MTT-treated cells are shown in D. *P* values were calculated by Student t-test. **(E)** *SRC* or scrambled SMARTpool siRNA-transfected PC3M cells were cultured in olaparib (3.0 μM) or talazoparib (0.03 μM) supplemented medium for 4 days post-transfection. The equivalent volume of DMSO was used as a placebo treatment. Cell viability (± SD) was measured by MTT assay. *P* values determined by Student's t-test. **(F)** PC3M cells that transiently overexpressed Y527F SRC (constitutively active SRC) were treated with olaparib (3.0 μM) or talazoparib (0.03 μM) for 7 days. Control cells were transfected with GFP expressing empty vector. Viability (± SD) of cells at 7 days as determined by MTT assay is shown. *P* values determined by Student's t-test.

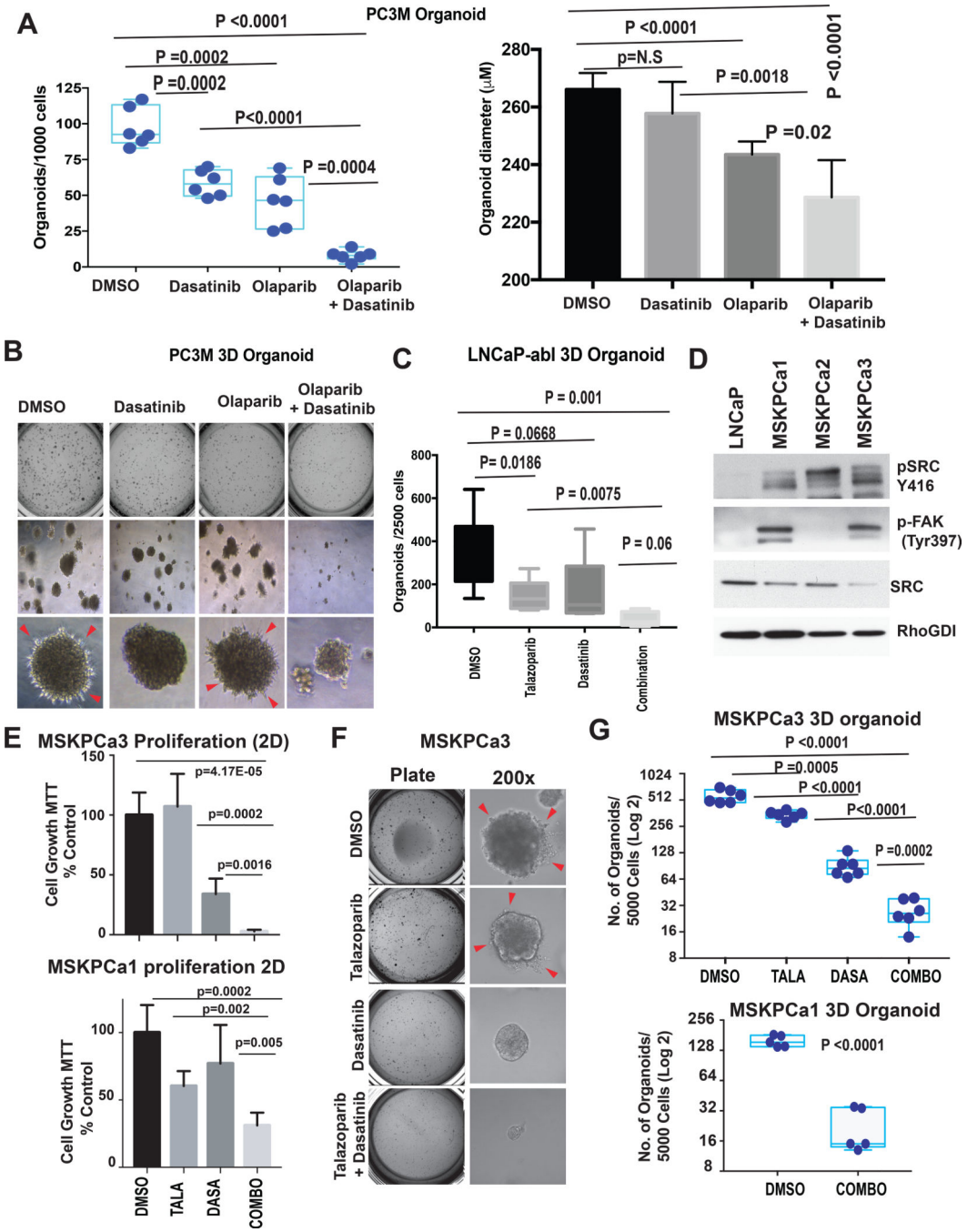

Figure 6. Synergistic effect of dasatinib and PARPi on 3D prostate cancer organoid growth

(A) PC3M cells (10^3 cells/well) were mixed with Matrigel, and 3D cell cultures (organoids) were grown in growth factor–enriched media. (See Supplementary Fig. S6A for schematic representation.) The number of 3D organoids (>200 µM diameter, ± SD) is shown. Each point represents the number of organoids (A) and average diameter of PC3M 3D organoids in (B) grown from 10^3 cells in each well. *P* value determined by Student's t-test. **(B)** Top, images of wells plate at Day 21. Middle, organoids at 40X magnification. Bottom, organoids at 100X magnification. Cells invading through Matrigel are indicated by arrows. **(C)**

Average number of 3D organoids (> 100 μM diameter, ± SD) derived from LNCaP-abl cells (plated at 5×10^3 cells/well). *P* value determined by Student's t-test. **(D)** Activation of SRC-FAK pathway in mCRPC-derived organoids (MSKPCa1–3) were analyzed by western blot using indicated antibodies. Lysate from parental LNCaP cells was used as cell line control. RhoGDI was used as loading control **(E)** Organoids (MSKPCa1 [bottom] and MSKPCa 3 [top]) were counted and plated to collagen-coated (Collagen I 50 μg/ml) 96-well plates (5000 cells/well in 100 μL media) and treated with dasatinib (0.3 μM) and talazoparib (0.03 μM) alone or in combination. The equivalent volume of DMSO was used as a placebo treatment. After 10 days, cells were treated with 0.5 mg/mL MTT. The graphs represent the inhibition of cell viability by single and combination treatment. *P* values were calculated by Student t-test. **(F)** MSKPCa3 cells (5×10^3 cells/well) were mixed with Matrigel, and 3D cell cultures (organoids) were grown in growth factor–enriched media and treated with dasatinib (0.3 μM) and talazoparib (0.03 μM) alone or in combination. Left, images of MSKPCa3 cell-derived 3D organoid in 24-well plate at Day 21. Right, organoids at 200X magnification. Cells invading through Matrigel are indicated by arrows. **(G)** The number of 3D organoids (>150 μM diameter, ± SD) derived from MSKPCa3 (top) and MSKPCa1 (bottom) are shown. Each point represents the number of organoids grown from 5×10^3 cells in each well of 24-well plate (after 4 weeks of plating the cells). *P* value determined by Student's t-test.